REPRODUCTION
REVIEW

What can we learn from gene expression profiling of mouse oocytes?

Toshio Hamatani[1,2], Mitsutoshi Yamada[1,2], Hidenori Akutsu[2], Naoaki Kuji[1], Yoshiyuki Mochimaru[1], Mitsuko Takano[1], Masashi Toyoda[2], Kenji Miyado[2], Akihiro Umezawa[2] and Yasunori Yoshimura[1]

[1]*Department of Obstetrics and Gynecology, Keio University School of Medicine, 35 Shinanomachi Shijuku-ku, Tokyo 160-8582, Japan and* [2]*Department of Reproductive Biology and Pathology, National Institute for Child Health and Development, 2-10-1 Okura Setagaya-ku, Tokyo 157-8535, Japan*

Correspondence should be addressed to T Hamatani; Email: t-hama@sc.itc.keio.ac.jp

Abstract

Mammalian ooplasm supports the preimplantation development and reprograms the introduced nucleus transferred from a somatic cell to confer pluripotency in a cloning experiment. However, the underlying molecular mechanisms of oocyte competence remain unknown. Recent advances in microarray technologies have allowed gene expression profiling of such tiny specimens as oocytes and preimplantation embryos, generating a flood of information about gene expressions. So, what can we learn from it? Here, we review the initiative global gene expression studies of mouse and/or human oocytes, focusing on the lists of maternal transcripts and their expression patterns during oogenesis and preimplantation development. Especially, the genes expressed exclusively in oocytes should contribute to the uniqueness of oocyte competence, driving mammalian development systems of oocytes and preimplantation embryos. Furthermore, we discuss future directions for oocyte gene expression profiling, including discovering biomarkers of oocyte quality and exploiting the microarray data for 'making oocytes'.

Reproduction (2008) **135** 581–592

Introduction

The mammalian oocyte is marked by extraordinary biological competence; it can haploidize its DNA, be fertilized and reprogram the sperm chromatin into a functional pronucleus, induce zygotic genome activation (ZGA), give rise to totipotency, and drive early embryonic development. Using its ability to reprogram a somatic nucleus transferred into an enucleated oocyte, derivation of embryonic stem (ES) cells from cloned blastocysts for therapeutic cloning is explored. The molecular mechanisms underlining such oocyte competence are largely unknown.

On the other hand, the reproductive capacity of women declines dramatically beyond the mid-30s (van Kooij *et al.* 1996, ASRM/SART 2000, Armstrong 2001, Klein & Sauer 2001), which is mainly caused by age-related decline in oocyte quality. For example, young women undergoing standard *in vitro* fertilization (IVF) with their own eggs show a success rate comparable with older women (>40 years) undergoing IVF with eggs donated by this younger subset of women (Navot *et al.* 1991). To overcome age-related decline in oocyte quality, ooplasmic donation has been performed by injecting ooplasm from a young, healthy donor oocyte into a patient oocyte to improve the outcome of assisted reproduction techniques (Cohen *et al.* 1997, 1998, Takeuchi *et al.* 1999). There is, however, little molecular evidence supporting the efficacy and the safety of ooplasmic donation. Furthermore, no molecular biomarker for oocyte quality has been established. Oocyte quality based on a morphological grading system is the only reliable prognostic factor in human IVF programs. Studies of molecular mechanisms involved in oocyte quality could have important implications for the efficacy and safety of clinical ooplasmic donation.

Thus, understanding the molecular mechanisms in oocytes is quite important for both reproductive biology and regenerative medicine. The scarcity of the materials, however, both in size (diameter <100 um) and in quantity (only a few to tens of oocytes from each ovulation in mice), has hampered the molecular analysis of oocytes. Earlier attempts to analyze oocytes employed RT-PCR and differential display using only a few candidate genes. In addition, serial analysis of gene expression (SAGE) and cDNA libraries were generated from mouse and human oocytes, and SAGE tags and expressed sequence tags (ESTs) were sequenced for rapid gene discovery and expression profiling in oocytes

ISSN 1470-1626 (paper) 1741-7899 (online)

DOI: 10.1530/REP-07-0430
Online version via www.reproduction-online.org

(Ko *et al.* 2000, Ko 2004, Adjaye 2005, Evsikov *et al.* 2006). Furthermore, the recent progress in RNA amplification methods and microarray platforms including genes unique to oocytes and preimplantation embryos allows us to apply global gene expression profiling to the studies of the oocytes and preimplantation embryos (Carter *et al.* 2003). To date, several reports of the oocyte transcriptome using unique biological models have been published (Dobson *et al.* 2004, Hamatani *et al.* 2004*a*, 2004*b*, Wang *et al.* 2004, Zeng *et al.* 2004, Pan *et al.* 2005, Assou *et al.* 2006, Kocabas *et al.* 2006, Yoon *et al.* 2006). The identification of a large number of genes expressed in oocytes, especially oocyte-specific genes, and multiple signaling pathways in the models by such global gene expression profiling is the first step toward understanding oocyte quality and the molecular mechanisms underlying oogenesis, developmental programs, and totipotency in preimplantation embryos.

Global gene expression profiling of mouse preimplantation embryos to dissect maternal transcripts

Two groups simultaneously published the first reports on global gene expression profiling of all stages of preimplantation embryos (Fig. 1; Hamatani *et al.* 2004*a*, Wang *et al.* 2004). While Wang *et al.* used the Affymetrix 25-mer oligo DNA microarray system, we used the NIA 60-mer oligo microarray (Agilent Mouse Development Array), which is enriched for genes expressed in stem cells and preimplantation embryos (Carter *et al.* 2003). Taking advantage of 60-mer oligo DNA hybridization kinetics (Hughes *et al.* 2001), it was also optimized for use with tiny amounts of RNA (Carter *et al.* 2003). During preimplantation development, 12 179 out of 21 939 gene features on the NIA 60-mer oligo microarray showed statistically significant changes with false discovery rate (FDR) $<10\%$ by ANOVA-FDR test. Pair-wise comparison, hierarchical clustering analysis, and principal component analysis (PCA) revealed two major transient waves of *de novo* transcription (Fig. 1A–C). The first wave corresponds to ZGA. The second wave, mid-preimplantation gene activation (MGA), contributes to dramatic morphological changes during late preimplantation development.

To trace the expression changes of individual genes, 12 179 statistically significant genes were analyzed by *k*-means clustering method and 9 clusters were identified (Fig. 2). Gene expression patterns of these clusters can be assigned to three main groups. The first group appears to represent ZGA genes that are first activated from the zygotic genome (Clusters 1, 4, 5, and 8). The list of the ZGA genes suggests that ZGA is not promiscuous as previously proposed and contributes mainly to the preparation of basic cellular machinery during the two-cell and the four-cell stages.

The second group represents maternal transcripts with distinctive patterns of degradation during preimplantation development (Clusters 7 and 9). Although the massive maternal RNA degradation pattern by the two-cell stage is confirmed (Cluster 9) as previous studies suggested (Nothias *et al.* 1995, Schultz 2002), 70.5 and 32.5% of the transcripts in Clusters 7 and 9 respectively further show significant reduction from the four-cell to eight-cell stages. Selective degradation of maternal transcripts during oocyte maturation is, as also shown by the latest study (Su *et al.* 2007), a developmentally regulated event preceding the transition of gene expression from maternal to zygotic control. Since most genes in Clusters 7 and 9 are not reactivated during preimplantation development, the genes in these clusters are suggested to have specific functions either in oogenesis, oocyte maturation, fertilization, and/or early phases of preimplantation development.

The third group appears to represent genes that follow a combination of these two patterns (Clusters 2 and 3); 3329 genes whose expression first significantly increase from the four-cell to eight-cell stages are identified as the MGA genes, and 82.7 and 12.3% of them fall into Clusters 2 and 3 respectively. Further expression profiling of embryos treated with inhibitors of transcription and translation reveals that the translation of maternal RNAs is required for the initiation of ZGA, suggesting a cascade of gene activation from maternal RNA/protein sets to ZGA gene sets and thence to MGA gene sets (Hamatani *et al.* 2004*a*).

By MAPPFinder (Dahlquist *et al.* 2002, Doniger *et al.* 2003), which is a tool to identify global biological trends in gene expression data by interacting the annotations of Gene Ontology (GO) terms (Ashburner *et al.* 2000), the genes in the clusters of maternal transcripts are associated to such GO terms as 'circadian rhythm,' 'M-phase of mitotic cell cycle,' 'DNA replication,' 'Golgi apparatus/intracellular protein transport,' 'adherent junction,' 'small GTPase regulatory/interacting protein,' and 'intracellular signaling cascade'. The 'circadian rhythm' category includes seven mammal known circadian genes: *Per1–3*, *Cry1–2*, *Bmal1/Arntl*, and *Clock*. The transcripts of *Bmal1/Arntl*, *Clock*, *Timeless*, *Cry1*, and *Csnk1e* decrease during the one-cell to two-cell stages as previous reports showed (Johnson *et al.* 2002).

The egg–sperm fusion at fertilization in mammals releases an oocyte from metaphase II arrest by increasing Ca^{2+} levels, activating Ca^{2+}-calmodulin kinase II, and targeting cyclin B and c-mos for degradation via the ubiquitin–proteasome pathway. *Rfpl4*, an E3 ubiquitin protein ligase, regulates the degradation of cyclin B1 (*Ccnb1*) protein (Cluster 6b) (Suzumori *et al.* 2003), which is a well-known example of a transcript with a short poly(A) tail that is regulated at the post-transcriptional level in oocytes. Furthermore, *Cpeb*, *Eif4e*, *Cpsf2*, and *Stk13/Aurkc*, which are involved in the masking and/or translational regulation of transcripts with short

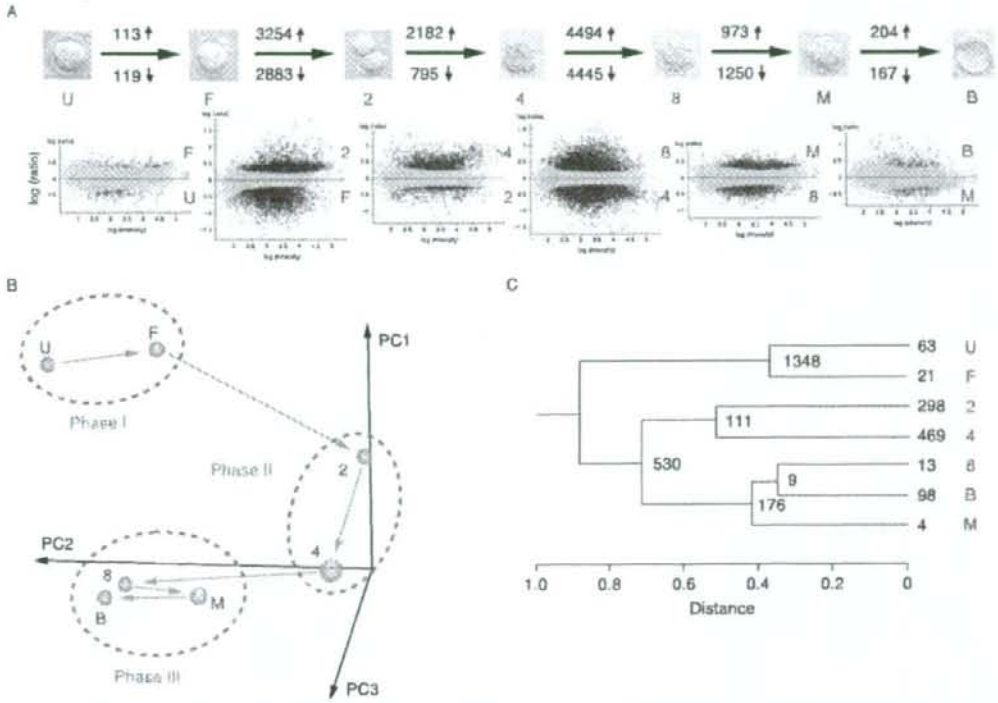

Figure 1 Global outlook of gene expression during preimplantation development (reprinted from 'Dynamics of global gene expression changes during mouse preimplantation development', Hamatani T *et al.* 2004 *Developmental Cell* **6** 117–131, with permission from Elsevier). (A) A matrix of scatter plots. U, F, 2, 4, 8, M, and B denote unfertilized egg, fertilized egg, two-cell embryo, four-cell embryo, eight-cell embryo, morula, and blastocyst respectively. Each scatter plot shows the comparison of gene expression between embryo stages. A horizontal axis represents the averaged log (intensity) of genes, whereas a vertical axis represents the log (ratio) of signal intensity for each gene between one stage and another stage. Colored spots (red and green) represent genes that passed the FDR = 10% statistical test. Red spots represent array features with higher expression at a later stage, whereas green spots represent array features with lower expression. (B) Principal component analysis. (C) Hierarchical clustering analysis. Numerical values represent the number of genes specific to each cluster or stage. A list of these stage-specific genes are available at the web site of Cell Press (Hamatani *et al.* 2004a).

poly(A) tails in oocytes (Hodgman *et al.* 2001, Mendez & Richter 2001), also decrease their transcripts by the two-cell stage. The presence of the 'DNA replication' category in oocytes indicates that oocytes are already well equipped with DNA replication machinery, as exemplified by the fact that neither the lack of *Zar1* (Wu *et al.* 2003) nor the presence of jasplakinolide, which is the most powerful known microfilament inhibitor (Terada *et al.* 2000), can prevent the initiation of DNA replication. In another global gene expression study of preimplantation embryos, DNA repair genes are also over-represented at the oocyte stage when compared with the one-cell through the blastocyst stages in their transcript profiling during preimplantation development (Zeng *et al.* 2004). Genes that are down-regulated from oocytes to two-cell embryos include many genes involved in DNA repairs, including *Orc1l, Orc4l, Orc5l, Orc6l, Mcm4, Pcna, Pola2, Polm, Blm, Top1*, and *Msh6* (Cluster 9); *Msh3* and *Mcm7* (Cluster 7); and *Cdc7l1/Cdc7, Cdc45l, Ccna2*, and *Dbf4/Ask* (Cluster 6). Furthermore, another group searched for maternal transcripts of polarity-regulating genes in mouse oocytes by global gene expression profiling of preimplantation embryos, which may subsequently control polarity in preimplantation embryos (Wang *et al.* 2004). They focused on three genes whose homologs have been shown to regulate cellular polarity in *Drosophila*: *Flamingo*, dystroglycan1 (*Dag1*), and cornichon (*Cnih2*) both of which are included by Cluster 3.

Global gene expression changes during oogenesis

Although several groups have studied global gene expression in human and mouse oocytes at the later stages of folliculogenesis (germinal vesicle stage and metaphase II stage; Wang *et al.* 2004, Cui *et al.* 2007,

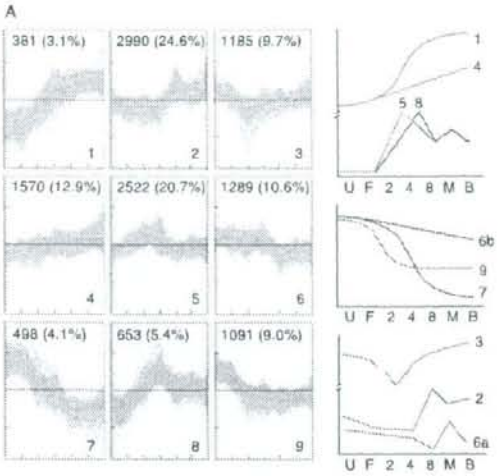

B

Cluster 6	Cluster 7	Cluster 9
Mater	Gdf9	Mos/c-mos
Ddx4/Vasa	Obox1	Kit/c-kit
Zp3	Ezh2	Stat3
Gata4	Mad2l2	Cry1
Frap1/mTOR	Tcl1	Oosp1
Fsrg1/Brd2	Bmi1	Noboxl/Og2x
Baz1a	Bmal1/Arntl	Cpeb1
Cdc45l	Clock	Magoh
Ilk	Zar1	Catna1
Dtr/HB-EGF	Rfpl4	N-cadherin
Smarca5	Mek1/Map2k1	Rac1
Brd4	Eps8	Hells/Lysh
Son	Stk13/AurkC	Mort4l2/MrgX
Nfkbia/IkBa	Zfp68	Baz1b
Nfkb1/NF-kB	Rnf35/2cz61	Zp1
	Sfmbt1	Zp2
	Spindlin	Scml2

Figure 2 Time-course analysis of individual genes. (Reprinted from 'Dynamics of global gene expression changes during mouse preimplantation development', Hamatani T *et al.* 2004 *Developmental Cell* **6** 117–131, with permission from Elsevier). (A) General trends of expression changes analyzed by *k*-means clustering method. The nine clusters were further classified into three super groups by visual inspection as shown in the three schemes in the far right column. (B) Representative genes in each cluster.

Gasca *et al.* 2007, Zhang *et al.* 2007), only two groups successfully performed global gene expression studies using mouse oocytes at the very early stages of folliculogenesis (Pan *et al.* 2005, Yoon *et al.* 2006). Pan *et al.* (2005) compared the transcriptomes of mouse oocytes obtained from day 2 primordial follicles to day 22 equine CG primed large antral follicles. From the primordial to large antral stages, 18 529 probe sets corresponding to 11 766 unigenes detected significant gene expression in oocytes that developed *in vivo*. The hierarchical clustering dendrogram and PCA analysis showed that the primordial oocyte is separated from oocytes obtained from the other stages. Many important genes encoding 'secreted proteins', which are defined on their own terms in that manuscript, display marked upregulation between the primordial and primary follicle stages (e.g., *Gdf9, Bmp15, Bmp5, Bmp6, Tgfb2, Tgfb3,* and several genes related to *Notch, Shh,* and *Egf* signaling pathways). Thus, the primordial to primary follicle transition is a major transition and likely reflects the dramatic reorganization in follicle structure and initiation of growth and development. Of the 16 883 probe sets differentially detected between these stages, 5020 display a twofold change in relative abundance. Another apparent transition occurs between oocytes obtained from secondary follicles and those from small antral follicles, which corresponds to the acquisition of meiotic competence. The 736 probe sets of which ~65% are downregulated display a significant twofold change at this transition.

The principal component-based clustering shows three distinct patterns of gene expression. The first pattern shows consistent increase or decrease throughout the oocyte development and the most dramatic changes from the primordial to primary follicle stages, which the bulk of genes (10 117 probe sets) display (Fig. 3A). The second pattern peaks or hits the bottom at the primary follicle stage (Fig. 3B) and the third one shows the dynamic expression changes from the primary to the secondary follicle stages (Fig. 3C). The Expression Analysis Systematic Explorer software (http://david.abcc.ncifcrf.gov/ease/ease.jsp) for discovery of biological themes within the list of genes also shows the overrepresentation of genes involved in DNA repair and response to DNA damage throughout oocyte development, suggesting a protective mechanism to insure genomic integrity of the female germ line.

In addition, by analysis of global gene expression profiling of oocytes during the germinal vesicle stage to the metaphase II stage, new potential regulators and marker genes for oocyte maturation have been identified: *Pacsin2, Map2k* (Cui *et al.* 2007), and the genes related to BRCA1 regulation pathway, including *Bard1, Rbbp4, Brap, Rbbp7, Rbl2, Bub3,* and *Bub1b* (Gasca *et al.* 2007).

Global gene expression changes during loss of oocyte quality

To elucidate factors determining oocyte quality, a mouse model highlighting the age-related decline in fertility and oocyte quality was used (Hamatani *et al.* 2004*b*, Steuerwald *et al.* 2007). The expression profiles of metaphase II oocytes collected from 5- to 6-week-old mice were compared with those collected from 42- to 45-week-old mice using the NIA 60-mer oligo microarray (Hamatani *et al.* 2004*b*). Among ~11 000 genes whose transcripts were detected in oocytes, about 5% (530) showed statistically significant expression changes,

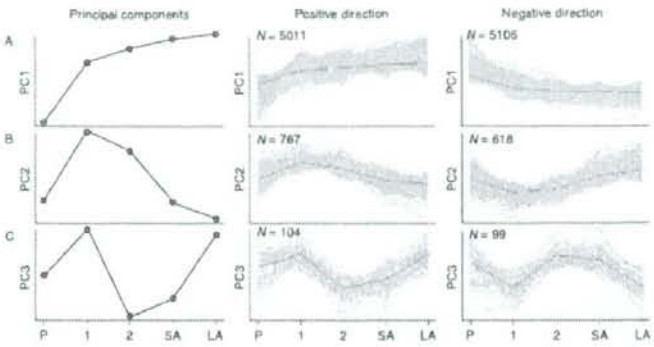

Figure 3 Principal component-based clustering to analyze gene expression profiles of oocytes during the primordial follicle stage to the large antral follicle stage (Pan *et al.* 2005) by NIA array analysis tool (http://lgsun.grc.nia.nih.gov/ANOVA/). The NIA Array Analysis tool identifies two clusters associated with a given pattern: genes positively and negatively correlated with the pattern. P, 1, 2, SA, and LA represent the primordial follicle stage, the primary follicle stage, the secondary follicle stage, the small antral follicle stage, and the large antral follicle stage respectively.

excluding the possibility of global decline in transcript abundance. Consistent with the generally accepted view of aging, the differentially expressed genes include ones involved in mitochondrial function and oxidative stress. Interestingly, a new non-invasive and highly sensitive method for measuring cellular respiration with scanning electrochemical microscopy shows that decreased cellular respiration in oocytes from aged mice is associated with impaired preimplantation development (Abe 2007). However, the expression of other genes involved in chromatin structure, DNA methylation, genome stability, and RNA helicases are also altered, suggesting the existence of additional mechanisms for aging in oocytes. For example, the decreased *Dnmt1* (*Dnmt1o* and *Dnmt1s*) expression and the increased *Dnmt3b* during aging are observed in oocytes. Because the same pattern of expression change in *Dnmt* genes has already been reported in aging WI-38 fibroblast cells (Lopatina *et al.* 2002), the genomic methylation patterns are suggested to be altered in aging cells. Telomerase reverse transcriptase and yeast mutant H/L/S mismatch repair gene homologs are also downregulated during aging. Interestingly, more than 30 zinc finger proteins are shown as the downregulated genes during aging. Furthermore, we identified and characterized a group of new oocyte-specific mouse genes, members of the human NACHT, leucine rich repeat and pyrin domain containing (*NALP/NLRP*) gene family among the transcripts decreased with aging. The *Nalp* gene family includes *Mater/Nalp5/Nlrp5* whose null mutant embryos arrest cleavage at the two-cell stage (Tong *et al.* 2000), suggesting an important role of this gene family in oogenesis, fertilization, and/or preimplantation development. These results have implications for aging research as well as for clinical ooplasmic donation to rejuvenate aging oocytes.

Polycystic ovary syndrome (PCOS) is another good model for studying loss of oocyte quality. The reproductive performance of women undergoing IVF treatment with PCOS is characterized by their good response to ovarian stimulation that yields higher number of oocytes; however, with lower implantation and higher miscarriage rates (Engmann *et al.* 1999, Ludwig *et al.* 1999, Mulders *et al.* 2003). Individual oocytes retrieved from nine women with PCOS and that from ten non-hirsute ovulatory women are used for microarray hybridization (Wood *et al.* 2007). Of the 8123 transcripts expressed in metaphase II oocytes, 374 show significant differences in mRNA abundance in the PCOS oocyte. The genes associated with chromosome alignment and centrosome, and the genes containing putative androgen receptors and/or PPARγ-binding sites are upregulated. The expression of these genes, which is generally not a part of the human oocyte transcriptome, is suggested to contribute to abnormalities in early embryonic development. Furthermore, upregulation of maternal-effect genes are notable. Although only seven mammalian maternal-effect genes (*Mater/Nlrp5*, *Hsf1*, *Dnmt1*, *Zar1*, *Npm2*, *Stella*, *Fmn2*, and *Bnc1*) have been identified to date, three (*Mater/Nlrp5*, *Fmn2*, and *Bnc1*) are upregulated. Increased expression of maternal-effect genes may negatively impact embryonic development.

Dielectrophoresis is a potential non-invasive method to select oocytes of good quality. In fact, dielectrophoretically separated *in vitro*-derived bovine metaphase II oocytes show a difference in the rate of blastocyst development and significant difference in transcriptional abundance of 36 genes as a result from global gene expression profiling. This suggests that dielectrophoretic behavior and the 36 genes including *Anxa2*, *Ptgs2*, and *Dnmt1* are potential biomarkers for oocyte quality (Dessie *et al.* 2007).

Recently, microarray technology was also applied to screening for chromosomal anomalies: comparative genomic hybridization (CGH) is used to assess the copy number of chromosomes in polar bodies and oocytes (Wells *et al.* 2002, Fragouli *et al.* 2006). CGH has the major advantage that every chromosome is tested, rather than the limited subset assessed using fluorescence *in situ* hybridization (FISH). The CGH protocols, which allow efficient DNA amplification from single cells and

reduce the amount of time required for the analysis, are currently undergoing preclinical testing in a number of preimplantation genetic diagnosis laboratories (Patrizio *et al.* 2007).

Identification of oocyte-specific transcripts and their clustering in the mouse genome

A mammalian oocyte is the only known cell that can activate a zygotic genome after fertilization and reprogram a somatic nucleus transferred from a differentiated cell in cloning experiments. Therefore, several genes specifically expressed in oocytes are likely responsible for the ability to reprogram genomes as well as for oogenesis. It is the case for the so-called maternal genes such as *Mater*, *Zar1*, and *Npm2* that are all required for normal embryonic development beyond the one-cell or two-cell stage (Fig. 4A; Tong *et al.* 2000, Dean 2002, Burns *et al.* 2003, Wu *et al.* 2003). *Gdf9* and *Bmp15* are also known to play important roles in female germ cells during folliculogenesis (Dong *et al.* 1996, Galloway *et al.* 2000). Accordingly, genes specifically expressed in the oocyte seem to control oogenesis, ovarian folliculogenesis, and preimplantation development.

In attempts to identify novel oocyte-specific genes, several groups have used mRNA differential display (Zeng & Schultz 2003), suppression subtractive hybridization (Hennebold *et al.* 2000), and *in silico* subtraction approaches (Rajkovic *et al.* 2001, Dade *et al.* 2003). It is, however, essential to analyze all transcripts/genes in a wide selection of organs and cell types including totipotent fertilized eggs, pluripotent embryonic cells, a variety of adult stem cells, and terminally differentiated cells. Sharov *et al.* (2003) obtained 249 200 high-quality EST sequences from the NCBI Unigene database that included a broad collection of NIA mouse cDNA libraries and clustered them into ~30 000 gene indexes including 977 previously unidentified genes. By analyzing the expression levels of the gene indexes based on the frequencies of the corresponding ESTs in Unigene cDNA libraries, genes that characterize oocytes and preimplantation embryos are identified (Sharov *et al.* 2003). Furthermore, the gene expression specificity to oocytes or/and preimplantation embryos is validated using gene expression profiling data of female germ cells during oogenesis and preimplantation embryos (Hamatani *et al.* 2004*a*, Wang *et al.* 2004, Pan *et al.* 2005). Several example of genes preferentially expressed in oocytes are selected and their gene expression levels are demonstrated to increase in oocytes during oogenesis (from the primordial follicle stage to the large antral follicle stage) and decrease during preimplantation development (from unfertilized egg to blastocyst) by the microarray experiments (Fig. 4B). Mager *et al.* (2006) also identified 51 genes as candidate maternal-effect genes *in silico* (always not present during the two-cell through the eight-cell or at the blastocyst stage), by comparing published results of three independent studies of mouse preimplantation embryo transcriptomes (Hamatani *et al.* 2004*a*, Wang *et al.* 2004, Zeng *et al.* 2004).

The group that found six genes of the mouse oogenesin family reported that not a few loci near the telomere in the mouse genome contain several genes specifically expressed in oocytes (Paillisson *et al.* 2005). Mouse oogenesin family genes are expressed exclusively in oocytes and present on chromosome 4 in a cluster of almost 1 Mb composed of 12 oogenesin paralogous genes. On the other hand, we also identified nine novel genes presenting similarities with *Mater/Nalp5* (Tong *et al.* 2000) and expression specific to oocytes, seven of which are clusterized on a certain locus of chromosome 7 (Fig. 5). The gene expression specificity of the novel Nalp-family genes to oocytes has been experimentally validated using Northern blot and *in situ* hybridization (Hamatani *et al.* 2004*b*; Fig. 6). Recently, we further identified a group of oocyte-specific genes encoding zinc finger proteins that clusterize in a near-telomere locus of chromosomes 6 and 11 (unpublished data). Telomeric regions of chromosomes are mainly composed of heterochromatin in most eukaryotic genomes. Because gene silencing near the telomere has been known and called 'telomere position effect' in *Drosophila* and yeast, the specific near-telomere position of the clusters of oocyte-specific genes in mice may contribute toward their gene silencing in non-ovarian tissues.

There is another noted attempt to identify important genes that are preferentially expressed in oocytes and conserved in chordates. Evsikov *et al.* (2006) compared the collection of ESTs from their mouse oocyte libraries to those from the eggs of *Xenopus* and ascidians to extract conserved genes that are expressed in chordate oocytes. More than 50% of the genes expressed in mouse oocyte libraries are also expressed in the eggs of *Xenopus* and ascidians. To investigate the evolutionary hardwired molecular pathways shared among chordates, GO term frequencies in 2090 genes that are commonly expressed in eggs of all three species are compared with those in the entire set of genes expressed in their mouse oocyte library. Although this analysis shows a substantial overlap with GO terms (biological process) associated with housekeeping genes, several GO terms (molecular function) such as 'motor activity,' 'small protein activating enzyme activity,' 'transferase activity,' 'helicase activity,' and two specific signal transducer activities (serine/threonine kinase activity and ligand-dependent nuclear receptor activity) are over-represented and provide a snapshot of gene functions shared particularly by the chordate oocytes. Another study group used a multi-species cDNA microarray containing 3456 transcripts from three distinct cDNA libraries from bovine, mouse, and *Xenopus* oocytes (Vallee *et al.* 2006). The cross-species hybridizations reveal that 1541 positive hybridization signals are generated by oocytes of all three species, and 268 of these, including *SMFN* (small fragment nuclease), *Spin* (spindlin), and

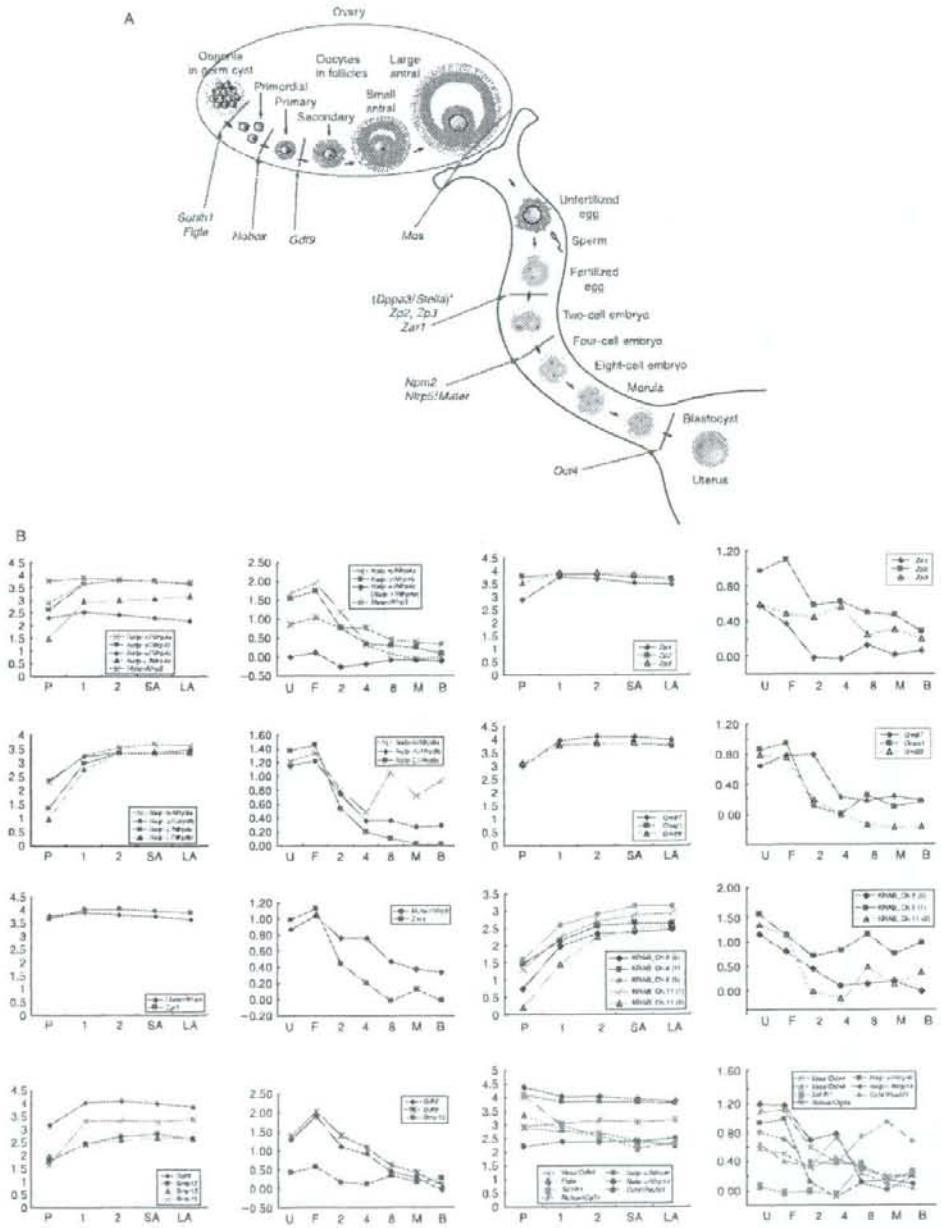

Figure 4 (A) Knockout mouse phenotypes of genes preferentially expressed in oocytes. *Development of embryos from *Stella*−/− intercrosses starts to be affected from 1.5 dpc onward (the two-cell stage) and only a low percentage reach the blastocyst stage by 3.5 dpc. (B) The gene expression changes of several genes known as oocyte specific. The oocyte-specific genes, including *Nalps*, showed increased expression during oogenesis and decreased expression during preimplantation development in the global gene expression studies. P, 1, 2, SA, and LA represent the primordial follicle stage, the primary follicle stage, the secondary follicle stage, the small antral follicle stage, and the large antral follicle stage respectively. U, F, 2, 4, 8, M, and B denote unfertilized egg, fertilized egg, two-cell embryo, four-cell embryo, eight-cell embryo, morula, and blastocyst respectively.

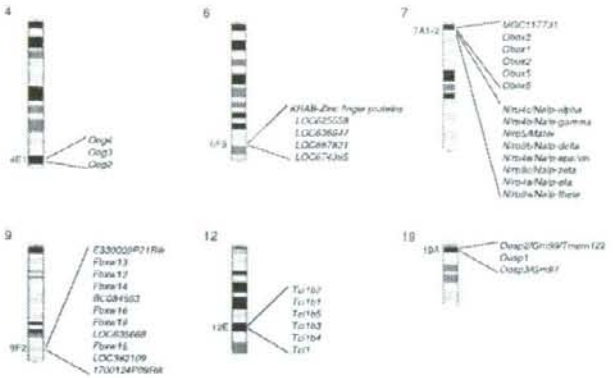

Figure 5 Clusters of oocyte-specific genes on mouse chromosomes 4, 6, 7, 9, 12, and 19.

PRMT1 (protein arginine methyltransferase 1) transcripts, are preferentially expressed in oocytes (Vallee *et al.* 2006). Furthermore, an important molecular characteristic of germ cells was also reported: germ cell-specific regulation of core promoter-associated transcription factors is conserved between *Xenopus* and mice (Xiao *et al.* 2006). *Tbpl2/Trf3* and *Gtf2a1l/Alf* are demonstrated to be expressed preferentially in oocytes and can form *in vitro* core promoter complexes with TBP and TFIIA. Therefore, identifying other germ cell-specific transcription factors is necessary to understand the genetic cascades that drive oocyte development and folliculogenesis.

Comparison of oocytes with ES cells in terms of their gene expression profiles

Recent studies on cell fusion between a somatic cell and an ES cell suggest that cytoplasm of ES cells can reprogram an introduced somatic nucleus to confer pluripotency. In this aspect, the cytoplasmic environments of ES cells and oocytes share the capacity to reprogram a somatic nucleus (Tada *et al.* 2001, Cowan *et al.* 2005). Accordingly, a set of genes commonly expressed in oocytes and ES cells are likely responsible for reprograming somatic cells. To identify these genes, gene expression profiling data of human oocytes and human ES cells were explored (Kocabas *et al.* 2006, Zhang *et al.* 2007). Compared with reference samples, 5331 and 1626 transcripts are significantly upregulated in human oocytes and ES cells respectively (Kocabas *et al.* 2006). When the genes differentially upregulated in human ES cells are intersected with those differentially upregulated in human oocytes, 388 transcripts are overlapped. This list of genes, including *POU5F1/OCT4*, *DNMT3b*, *DAZL*, and high-mobility group proteins (*HMGB2*, *HMGB3*, and *HMGN4*) (Kocabas *et al.* 2006), may provide good candidate genes for the future studies on molecular mechanisms of nuclear reprograming.

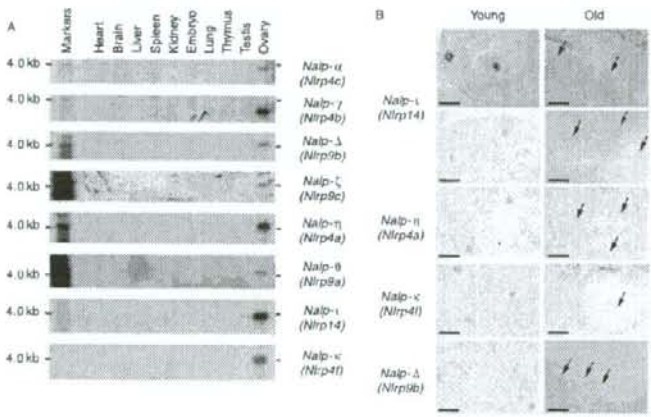

Figure 6 Oocyte-specific expression of the novel Nalp-family mouse genes (reprinted from 'Age-associated alteration of gene expression patterns in mouse oocytes', Hamatani T *et al.* 2004 *Human Molecular Genetics* **13** 2263–2278, with permission from Oxford University Press). (A) Northern blot analysis shows their ovary-specific expression and (B) *in situ* hybridization shows their oocyte-specific expression on ovary sections.

On the other hand, 'induced pluripotent stem cells (iPS cells)' were recently generated by forced expression of defined factors: *Pou5f1/Oct4*, *Sox2*, *Klf4*, and *Myc* (Takahashi & Yamanaka 2006). Surprisingly, iPS cells selected by Nanog expression are capable of germ cell transmission (Okita *et al.* 2007). These iPS factors, however, show little maternal expression in oocytes (except in the case of *Oct4*) and increased zygotic expression during preimplantation stages (except in the case of *Myc*), based on EST frequencies in Unigene cDNA libraries and microarray data during oogenesis to preimplantation development (Fig. 7). Therefore, the mechanism of oocytes to induce pluripotency is likely different from that of ES cells. Although the genes commonly expressed in oocytes and ES cells are not necessarily important to induce pluripotency, maternal factors that can induce zygotic expression of the 'iPS factors' (*Oct4*, *Sox2*, and *Klf4*) are rather more substantial in oocytes.

Perspective

Oocytes offer a relatively homogeneous biological system that is well adapted to gene expression profiling studies: arrest of cell cycle at the metaphase II stage, quiescence in transcription after germinal vesicle breakdown, and little contamination in oocyte samples with any other types of cells after thorough removal of cumulus cells. There are, however, several limitations in applying microarray technologies to study the molecular mechanisms in oocytes and preimplantation embryos. Although the recent advent of linear RNA amplification (*in vitro* transcription-based protocols) and exponential amplification (PCR-based strategies) techniques allowed several groups to study oocyte transcriptomes using a tiny amount of RNA even in an individual oocyte (Bermudez *et al.* 2004, Dobson *et al.* 2004, Li *et al.* 2006, Jones *et al.* 2007), the efficacy of RNA amplification is not yet good enough to analyze an individual blastomere of preimplantation embryos. Furthermore, poly(A) length affects efficiency of RNA amplification. Although the synthesis of new transcripts essentially ceases after germinal vesicle breakdown, poly(A) tails of some classes of existing transcripts in oocytes are elongated, leading to increased translation and protein levels (Bachvarova 1992). Thus, regulation of the poly(A) tail length is a major mechanism for controlling maternal transcript activity. Unlike the T7-oligo(dT) primers used in the conventional linear RNA amplification procedures, the uniquely designed Full Spectrum MultiStart Primers for *in vitro* transcription from System Biosciences (Mountain View, CA, USA) initiates cDNA synthesis at multiple points along mRNAs with little or no bias with respect to the length of poly(A) tails. Transcript profiles generated from microarray studies using this modified RNA amplification protocol would provide a more accurate perspective of the

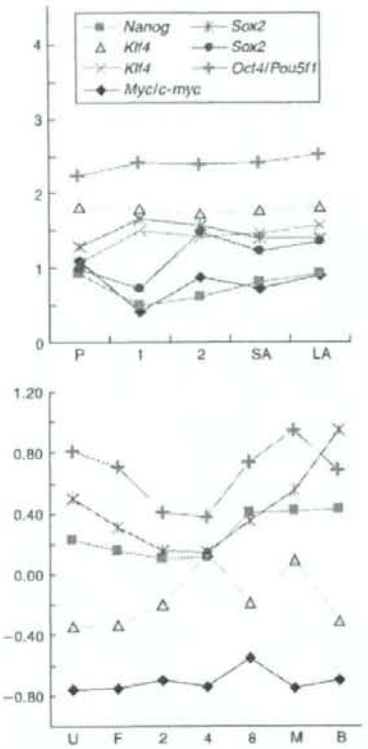

Figure 7 The gene expression changes of the iPS factors based on the published microarray data. P, 1, 2, SA, and LA represent the primordial follicle stage, the primary follicle stage, the secondary follicle stage, the small antral follicle stage, and the large antral follicle stage respectively. U, F, 2, 4, 8, M, and B denote unfertilized egg, fertilized egg, two-cell embryo, four-cell embryo, eight-cell embryo, morula, and blastocyst respectively.

global changes in populations of both degrading and stable transcripts during oocyte maturation and ZGA (Su *et al.* 2007).

'Tailor-made regenerative medicine' includes nuclear transfer from a patient's somatic cell to an enucleated donated oocyte, development of the reconstructed embryo up to the blastocyst stage, and establishment of the patient's ES cells. 'Making oocytes' will be an essential technique to develop 'tailor-made regenerative medicine' that needs large quantities of healthy ooplasms. 'Oocyte-like' cells were recently grown and isolated by utilizing GFP expression as a selection marker during differentiation of ES cells containing GFP expression cassettes under the *Pou5f1* promoter (Hubner *et al.* 2003). Nobody, however, has succeeded in generating oocytes by manipulating gene expression in ES and somatic cells. Even though forced expression of a set of several transcription factors in ES cells

may allow us to generate an oocyte, there is a problem in the oocyte; its nucleus ought to have genetic abnormalities. In contrast, its ooplasm might contain all the gene products that can support embryonic development after fertilization. Unlike another strategy using iPS cells that cannot avoid transmitting genetic abnormalities, the ooplasm can be safely used for 'tailor-made regenerative medicine' or 'ooplasmic donation'.

Since transcriptional cascades that activate an oocyte-specific developmental program are largely unknown, a set of master genes that drive the cascades have not yet been defined. Oocyte-specific transcription factors, however, are likely to be the critical switches for the differentiation into oocytes and good candidates for manipulation of gene expression. For example, NOBOX binds to the NOBOX binding elements with high affinity and augments transcriptional activity of mouse *Pou5f1* and *Gdf9* promoters (Choi & Rajkovic 2006). Other examples are factor in germ cell (FIGLA) and SOHLH1 that bind to E-box. They are suggested to increase transcriptional activity of *Zp1–3*, which have promoters including E-box (Yan *et al.* 2006: Pangas, 2006 #613).

On the other hand, nobody pays attention to a transcription factor whose knockout showed no distinctive phenotypes. Nonetheless, recent advent in microarray technologies allows us to catch any changes in a gene expression profile of cells transfected with a construct to modify gene expression. If a gene expression profile of ES cells approaches that of oocytes in the PCA coordinate, in spite of no phenotypic change, by upregulation of a certain transcription factor, the transcription factor is likely a candidate gene as a tool to induce the oocyte developmental program (Fig. 8). Further forced expression of another transcription factor in the ES cell may result in a similar gene expression profile to that of oocytes and then may achieve a certain remarkable phenotype including follicles or oocytes. Such synergy between cell biology and bioinformatics will become more important and beneficial to establish an *in vitro* oocyte-development model to 'make an oocyte'.

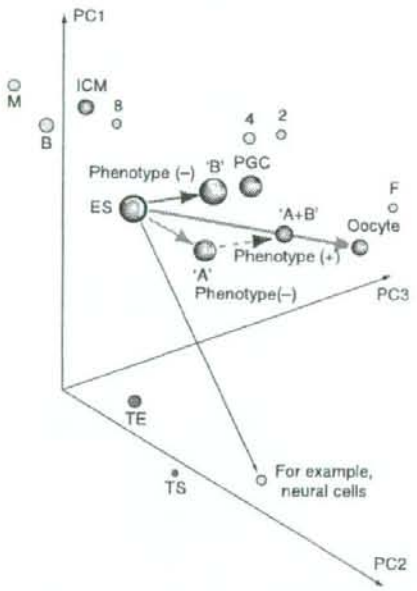

Figure 8 Explanation of a model to transform ES cells efficiently into oocytes using gene expression profiling as a guide. PC, principle component; PGC, primordial germ cell; ICM, inner cell mass; TE, trophectoderm; F, fertilized egg; 2, two-cell embryo; 4, four-cell embryo; 8, eight-cell embryo; M, morula; B, blastocyst. If over-expression of 'gene A' makes a global expression profile of ES cells closer to that of oocytes in the PCA coordinate, 'gene A' could be a good candidate to promote the oocyte developmental program. Even though no changes in phenotypes of ES cells are observed with over-expression of 'gene A', forced expression of 'gene A' plus that of 'gene B' in ES cells may show a distinctive phenotype including oocytes or follicles.

Acknowledgements

The authors declare that there is no conflict of interest that would prejudice the impartiality of this scientific work.

References

Abe H 2007 A non-invasive and sensitive method for measuring cellular respiration with a scanning electrochemical microscopy to evaluate embryo quality. *Journal of Mammalian Ova Research* **24** 70–78.

Adjaye J 2005 Whole-genome approaches for large-scale gene identification and expression analysis in mammalian preimplantation embryos. *Reproduction, Fertility, and Development* **17** 37–45.

Armstrong DT 2001 Effects of maternal age on oocyte developmental competence. *Theriogenology* **55** 1303–1322.

Ashburner M, Ball CA, Blake JA, Botstein D, Butler H, Cherry JM, Davis AP, Dolinski K, Dwight SS, Eppig JT, *et al.* 2000 Gene ontology: tool for the unification of biology. The Gene Ontology Consortium. *Nature Genetics* **25** 25–29.

ASRM/SART 2000 Assisted reproductive technology in the United States: 1997 results generated from the American Society for Reproductive Medicine/Society for Assisted Reproductive Technology Registry. *Fertility and Sterility* **74** 641–653 (discussion 653–644).

Assou S, Anahory T, Pantesco V, Le Carrour T, Pellestor F, Klein B, Reyftmann L, Dechaud H, De Vos J & Hamamah S 2006 The human cumulus–oocyte complex gene-expression profile. *Human Reproduction* **21** 1705–1719.

Bachvarova RF 1992 A maternal tail of poly(A): the long and the short of it. *Cell* **69** 895–897.

Bermudez MG, Wells D, Malter H, Munne S, Cohen J & Steuerwald NM 2004 Expression profiles of individual human oocytes using microarray technology. *Reproductive Biomedicine Online* **8** 325–337.

Burns KH, Viveiros MM, Ren Y, Wang P, DeMayo FJ, Frail DE, Eppig JJ & Matzuk MM 2003 Roles of NPM2 in chromatin and nucleolar organization in oocytes and embryos. *Science* **300** 633–636.

Carter MG, Hamatani T, Sharov AA, Carmack CE, Qian Y, Aiba K, Ko NT, Dudekula DB, Brzoska PM, Hwang SS, *et al.* 2003 *In situ*-synthesized novel microarray optimized for mouse stem cell and early developmental expression profiling. *Genome Research* **13** 1011–1021.

Choi Y & Rajkovic A 2006 Characterization of NOBOX DNA binding specificity and its regulation of Gdf9 and Pou5f1 promoters. *Journal of Biological Chemistry* **281** 35747–35756.

Cohen J, Scott R, Schimmel T, Levron J & Willadsen S 1997 Birth of infant after transfer of anucleate donor oocyte cytoplasm into recipient eggs. *Lancet* **350** 186–187.

Cohen J, Scott R, Alikani M, Schimmel T, Munne S, Levron J, Wu L, Brenner C, Warner C & Willadsen S 1998 Ooplasmic transfer in mature human oocytes. *Molecular Human Reproduction* **4** 269–280.

Cowan CA, Atienza J, Melton DA & Eggan K 2005 Nuclear reprogramming of somatic cells after fusion with human embryonic stem cells. *Science* **309** 1369–1373.

Cui XS, Li XY, Yin XJ, Kong IK, Kang JJ & Kim NH 2007 Maternal gene transcription in mouse oocytes: genes implicated in oocyte maturation and fertilization. *Journal of Reproduction and Development* **53** 405–418.

Dade S, Callebaut I, Mermillod P & Monget P 2003 Identification of a new expanding family of genes characterized by atypical LRR domains. Localization of a cluster preferentially expressed in oocyte. *FEBS Letters* **555** 533–538.

Dahlquist KD, Salomonis N, Vranizan K, Lawlor SC & Conklin BR 2002 GenMAPP, a new tool for viewing and analyzing microarray data on biological pathways. *Nature Genetics* **31** 19–20.

Dean J 2002 Oocyte-specific genes regulate follicle formation, fertility and early mouse development. *Journal of Reproductive Immunology* **53** 171–180.

Dessie SW, Rings F, Holker M, Gilles M, Jennen D, Tholen E, Havlicek V, Besenfelder U, Sukhorukov VL, Zimmermann U, *et al.* 2007 Dielectrophoretic behavior of *in vitro*-derived bovine metaphase II oocytes and zygotes and its relation to *in vitro* embryonic developmental competence and mRNA expression pattern. *Reproduction* **133** 931–946.

Dobson AT, Raja R, Abeyta MJ, Taylor T, Shen S, Haqq C & Pera RA 2004 The unique transcriptome through day 3 of human preimplantation development. *Human Molecular Genetics* **13** 1461–1470.

Dong J, Albertini DF, Nishimori K, Kumar TR, Lu N & Matzuk MM 1996 Growth differentiation factor-9 is required during early ovarian folliculogenesis. *Nature* **383** 531–535.

Doniger SW, Salomonis N, Dahlquist KD, Vranizan K, Lawlor SC & Conklin BR 2003 MAPPFinder: using gene ontology and GenMAPP to create a global gene-expression profile from microarray data. *Genome Biology* **4** R7.

Engmann L, Maconochie N, Sladkevicius P, Bekir J, Campbell S & Tan SL 1999 The outcome of *in vitro* fertilization treatment in women with sonographic evidence of polycystic ovarian morphology. *Human Reproduction* **14** 167–171.

Evsikov AV, Graber JH, Brockman JM, Hampl A, Holbrook AE, Singh P, Eppig JJ, Solter D & Knowles BB 2006 Cracking the egg: molecular dynamics and evolutionary aspects of the transition from the fully grown oocyte to embryo. *Genes and Development* **20** 2713–2727.

Fragouli E, Wells D, Thornhill A, Serhal P, Faed MJ, Harper JC & Delhanty JD 2006 Comparative genomic hybridization analysis of human oocytes and polar bodies. *Human Reproduction* **21** 2319–2328.

Galloway SM, McNatty KP, Cambridge LM, Laitinen MP, Juengel JL, Jokiranta TS, McLaren RJ, Luiro K, Dodds KG, Montgomery GW, *et al.* 2000 Mutations in an oocyte-derived growth factor gene (BMP15) cause increased ovulation rate and infertility in a dosage-sensitive manner. *Nature Genetics* **25** 279–283.

Gasca S, Pellestor F, Assou S, Loup V, Anahory T, Dechaud H, De Vos J & Hamamah S 2007 Identifying new human oocyte marker genes: a microarray approach. *Reproductive Biomedicine Online* **14** 175–183.

Hamatani T, Carter MG, Sharov AA & Ko MS 2004*a* Dynamics of global gene expression changes during mouse preimplantation development. *Developmental Cell* **6** 117–131.

Hamatani T, Falco G, Carter MG, Akutsu H, Stagg CA, Sharov AA, Dudekula DB, VanBuren V & Ko MS 2004*b* Age-associated alteration of gene expression patterns in mouse oocytes. *Human Molecular Genetics* **13** 2263–2278.

Hennebold JD, Tanaka M, Saito J, Hanson BR & Adashi EY 2000 Ovary-selective genes I: the generation and characterization of an ovary-selective complementary deoxyribonucleic acid library. *Endocrinology* **141** 2725–2734.

Hodgman R, Tay J, Mendez R & Richter JD 2001 CPEB phosphorylation and cytoplasmic polyadenylation are catalyzed by the kinase IAK1/Eg2 in maturing mouse oocytes. *Development* **128** 2815–2822.

Hubner K, Fuhrmann G, Christenson LK, Kehler J, Reinbold R, De La Fuente R, Wood J, Strauss JF III, Boiani M & Scholer HR 2003 Derivation of oocytes from mouse embryonic stem cells. *Science* **300** 1251–1256.

Hughes TR, Mao M, Jones AR, Burchard J, Marton MJ, Shannon KW, Lefkowitz SM, Ziman M, Schelter JM, Meyer MR, *et al.* 2001 Expression profiling using microarrays fabricated by an ink-jet oligonucleotide synthesizer. *Nature Biotechnology* **19** 342–347.

Johnson MH, Lim A, Fernando D & Day ML 2002 Circadian clockwork genes are expressed in the reproductive tract and conceptus of the early pregnant mouse. *Reproductive Biomedicine Online* **4** 140–145.

Jones GM, Song B, Cram DS & Trounson AO 2007 Optimization of a microarray based approach for deriving representative gene expression profiles from human oocytes. *Molecular Reproduction and Development* **74** 8–17.

Klein J & Sauer MV 2001 Assessing fertility in women of advanced reproductive age. *American Journal of Obstetrics and Gynecology* **185** 758–770.

Ko MS 2004 Embryogenomics of pre-implantation mammalian development: current status. *Reproduction, Fertility, and Development* **16** 79–85.

Ko MS, Kitchen JR, Wang X, Threat TA, Hasegawa A, Sun T, Grahovac MJ, Kargul GJ, Lim MK, Cui Y, *et al.* 2000 Large-scale cDNA analysis reveals phased gene expression patterns during preimplantation mouse development. *Development* **127** 1737–1749.

Kocabas AM, Crosby J, Ross PJ, Otu HH, Beyhan Z, Can H, Tam WL, Rosa GJ, Halgren RG, Lim B, *et al.* 2006 The transcriptome of human oocytes. *PNAS* **103** 14027–14032.

van Kooij RJ, Looman CW, Habbema JD, Dorland M & te Velde E 1996 Age-dependent decrease in embryo implantation rate after *in vitro* fertilization. *Fertility and Sterility* **66** 769–775.

Li SS, Liu YH, Tseng CN & Singh S 2006 Analysis of gene expression in single human oocytes and preimplantation embryos. *Biochemical and Biophysical Research Communications* **340** 48–53.

Lopatina N, Haskell JF, Andrews LG, Poole JC, Saldanha S & Tollefsbol T 2002 Differential maintenance and de novo methylating activity by three DNA methyltransferases in aging and immortalized fibroblasts. *Journal of Cellular Biochemistry* **84** 324–334.

Ludwig M, Finas DF, al-Hasani S, Diedrich K & Ortmann O 1999 Oocyte quality and treatment outcome in intracytoplasmic sperm injection cycles of polycystic ovarian syndrome patients. *Human Reproduction* **14** 354–358.

Mager J, Schultz RM, Brunk BP & Bartolomei MS 2006 Identification of candidate maternal-effect genes through comparison of multiple microarray data sets. *Mammalian Genome* **17** 941–949.

Mendez R & Richter JD 2001 Translational control by CPEB: a means to the end. *Nature Reviews. Molecular Cell Biology* **2** 521–529.

Mulders AG, Laven JS, Imani B, Eijkemans MJ & Fauser BC 2003 IVF outcome in anovulatory infertility (WHO group 2) – including polycystic ovary syndrome – following previous unsuccessful ovulation induction. *Reproductive Biomedicine Online* **7** 50–58.

Navot D, Bergh PA, Williams MA, Garrisi GJ, Guzman I, Sandler B & Grunfeld L 1991 Poor oocyte quality rather than implantation failure as a cause of age-related decline in female fertility. *Lancet* **337** 1375–1377.

Nothias JY, Majumder S, Kaneko KJ & DePamphilis ML 1995 Regulation of gene expression at the beginning of mammalian development. *Journal of Biological Chemistry* **270** 22077–22080.

Okita K, Ichisaka T & Yamanaka S 2007 Generation of germline-competent induced pluripotent stem cells. *Nature* **448** 313–317.

Paillisson A, Dade S, Callebaut I, Bontoux M, Dalbies-Tran R, Vaiman D & Monget P 2005 Identification, characterization and metagenome analysis of oocyte-specific genes organized in clusters in the mouse genome. *BMC Genomics* **6** 76.

Pan H, O'Brien MJ, Wigglesworth K, Eppig JJ & Schultz RM 2005 Transcript profiling during mouse oocyte development and the effect of gonadotropin priming and development *in vitro*. *Developmental Biology* **286** 493–506.

Patrizio P, Fragouli E, Bianchi V, Borini A & Wells D 2007 Molecular methods for selection of the ideal oocyte. *Reproductive Biomedicine Online* **15** 346–353.

Rajkovic A, Yan MSC, Klysik M & Matzuk M 2001 Discovery of germ cell-specific transcripts by expressed sequence tag database analysis. *Fertility and Sterility* **76** 550–554.

Schultz RM 2002 The molecular foundations of the maternal to zygotic transition in the preimplantation embryo. *Human Reproduction Update* **8** 323–331.

Sharov AA, Piao Y, Matoba R, Dudekula DB, Qian Y, VanBuren V, Falco G, Martin PR, Stagg CA, Bassey UC, *et al.* 2003 Transcriptome analysis of mouse stem cells and early embryos. *PLoS Biology* **1** E74.

Steuerwald NM, Bermudez MG, Wells D, Munne S & Cohen J 2007 Maternal age-related differential global expression profiles observed in human oocytes. *Reproductive Biomedicine Online* **14** 700–708.

Su YQ, Sugiura K, Woo Y, Wigglesworth K, Kamdar S, Affourtit J & Eppig JJ 2007 Selective degradation of transcripts during meiotic maturation of mouse oocytes. *Developmental Biology* **302** 104–117.

Suzumori N, Burns KH, Yan W & Matzuk MM 2003 RFPL4 interacts with oocyte proteins of the ubiquitin-proteasome degradation pathway. *PNAS* **100** 550–555.

Tada M, Takahama Y, Abe K, Nakatsuji N & Tada T 2001 Nuclear reprogramming of somatic cells by *in vitro* hybridization with ES cells. *Current Biology* **11** 1553–1558.

Takahashi K & Yamanaka S 2006 Induction of pluripotent stem cells from mouse embryonic and adult fibroblast cultures by defined factors. *Cell* **126** 663–676.

Takeuchi T, Ergun B, Huang TH, Rosenwaks Z & Palermo GD 1999 A reliable technique of nuclear transplantation for immature mammalian oocytes. *Human Reproduction* **14** 1312–1317.

Terada Y, Simerly C & Schatten G 2000 Microfilament stabilization by jasplakinolide arrests oocyte maturation, cortical granule exocytosis, sperm incorporation cone resorption, and cell-cycle progression, but not DNA replication, during fertilization in mice. *Molecular Reproduction and Development* **56** 89–98.

Tong ZB, Gold L, Pfeifer KE, Dorward H, Lee E, Bondy CA, Dean J & Nelson LM 2000 Mater, a maternal effect gene required for early embryonic development in mice. *Nature Genetics* **26** 267–268.

Vallee M, Robert C, Methot S, Palin MF & Sirard MA 2006 Cross-species hybridizations on a multi-species cDNA microarray to identify evolutionarily conserved genes expressed in oocytes. *BMC Genomics* **7** 113.

Wang QT, Piotrowska K, Ciemerych MA, Milenkovic L, Scott MP, Davis RW & Zernicka-Goetz M 2004 A genome-wide study of gene activity reveals developmental signaling pathways in the preimplantation mouse embryo. *Developmental Cell* **6** 133–144.

Wells D, Escudero T, Levy B, Hirschhorn K, Delhanty JD & Munne S 2002 First clinical application of comparative genomic hybridization and polar body testing for preimplantation genetic diagnosis of aneuploidy. *Fertility and Sterility* **78** 543–549.

Wood JR, Dumesic DA, Abbott DH & Strauss JF III 2007 Molecular abnormalities in oocytes from women with polycystic ovary syndrome revealed by microarray analysis. *Journal of Clinical Endocrinology and Metabolism* **92** 705–713.

Wu X, Viveiros MM, Eppig JJ, Bai Y, Fitzpatrick SL & Matzuk MM 2003 Zygote arrest 1 (Zar1) is a novel maternal-effect gene critical for the oocyte-to-embryo transition. *Nature Genetics* **33** 187–191.

Xiao L, Kim M & DeJong J 2006 Developmental and cell type-specific regulation of core promoter transcription factors in germ cells of frogs and mice. *Gene Expression Patterns* **6** 409–419.

Yan C, Elvin JA, Lin YN, Hadsell LA, Wang J, DeMayo FJ & Matzuk MM 2006 Regulation of growth differentiation factor 9 expression in oocytes *in vivo*: a key role of the E-box. *Biology of Reproduction* **74** 999–1006.

Yoon SJ, Kim KH, Chung HM, Choi DH, Lee WS, Cha KY & Lee KA 2006 Gene expression profiling of early follicular development in primordial, primary, and secondary follicles. *Fertility and Sterility* **85** 193–203.

Zeng F & Schultz RM 2003 Gene expression in mouse oocytes and preimplantation embryos: use of suppression subtractive hybridization to identify oocyte- and embryo-specific genes. *Biology of Reproduction* **68** 31–39.

Zeng F, Baldwin DA & Schultz RM 2004 Transcript profiling during preimplantation mouse development. *Developmental Biology* **272** 483–496.

Zhang P, Kerkela E, Skottman H, Levkov L, Kivinen K, Lahesmaa R, Hovatta O & Kere J 2007 Distinct sets of developmentally regulated genes that are expressed by human oocytes and human embryonic stem cells. *Fertility and Sterility* **87** 677–690.

Received 22 September 2007
First decision 31 October 2007
Revised manuscript received 1 February 2008
Accepted 27 February 2008

The fusing ability of sperm is bestowed by CD9-containing vesicles released from eggs in mice

Kenji Miyado*†‡§, Keiichi Yoshida‡¶, Kazuo Yamagata‖, Keiichi Sakakibara*, Masaru Okabe**, Xiaobiao Wang*, Kiyoko Miyamoto*, Hidenori Akutsu*, Takahiko Kondo*, Yuji Takahashi*, Tadanobu Ban††, Chizuru Ito¶, Kiyotaka Toshimori¶, Akihiro Nakamura*, Masahiko Ito*, Mami Miyado*, Eisuke Mekada**, and Akihiro Umezawa*

*National Center for Child Health and Development, 2-10-1 Okura, Setagaya, Tokyo 157-8535, Japan; †School of Biomedical Science, Tokyo Medical and Dental University, Yushima, Bunkyo, Tokyo 113-8510, Japan; ¶Graduate School of Medicine, Chiba University, 1-8-1 Inohana, Chuo-ku, Chiba 260-8670, Japan; ‖Center for Developmental Biology, RIKEN Kobe Institute, 2-2-3 Minatojima-minamimachi, Chuo-ku, Kobe, Hyogo 650-0047, Japan; and **Research Institute for Microbial Diseases, and ††Faculty of Medicine, Osaka University, 3-1 Yamadaoka, Suita, Osaka 565-0871, Japan

Edited by Ryuzo Yanagimachi, University of Hawaii, Honolulu, HI, and approved July 8, 2008 (received for review November 8, 2007)

Membrane fusion is an essential step in the encounter of two nuclei from sex cells—sperm and egg—in fertilization. However, aside from the involvement of two molecules, CD9 and Izumo, the mechanism of fusion remains unclear. Here, we show that sperm–egg fusion is mediated by vesicles containing CD9 that are released from the egg and interact with sperm. We demonstrate that the $CD9^{-/-}$ eggs, which have a defective sperm-fusing ability, have impaired release of CD9-containing vesicles. We investigate the fusion-facilitating activity of CD9-containing vesicles by examining the fusion of sperm to $CD9^{-/-}$ eggs with the aid of exogenous CD9-containing vesicles. Moreover, we show, by examining the fusion of sperm to $CD9^{-/-}$ eggs, that hamster eggs have a similar fusing ability as mouse eggs. The CD9-containing vesicle release from unfertilized eggs provides insight into the mechanism required for fusion with sperm.

fertilization | membrane fusion | EGFP | exosome

Fertilization is an essential process that naturally produces a cell capable of developing into a new individual. It consists of sequential events, including membrane fusion of sperm and egg (1). Despite the importance of understanding fertilization in controlling human reproduction and preserving endangered species, the molecular basis underlying the fusion remains a mystery, however. Previously, we reported that a tetraspan-membrane protein (tetraspanin), CD9, is expressed on the egg plasma membrane and is required for sperm–egg fusion (2–4). A role of CD9 in other fusion events also has been demonstrated (5). When sperm are added to eggs from $CD9^{-/-}$ females, the sperm bind to the egg plasma membrane normally, but fusion is severely impaired (2–4). Two recent observations suggest that CD9 plays a role in the organization of egg membrane. First, CD9 is transferred from the egg to the fertilizing sperm present in the perivitelline space (PVS) (6), suggesting the involvement of a process similar to trogocytosis, a mechanism of cell-to-cell contact-dependent transfer of membrane fragments (7). Second, CD9 deficiency alters the length and density of microvilli on the egg plasma membrane (8). CD9 is also known to be a component of exosomes, membrane vesicles released from a wide range of cells (9, 10). Despite its relationship to CD9, the involvement of exosome release in sperm–egg fusion remains unknown. In the present study, we analyzed the potential of enhanced green fluorescent protein (EGFP)-tagged CD9 (CD9-EGFP) as a reporter protein to study sperm–egg fusion in living mouse eggs.

Results

To observe the movement of CD9 during sperm–egg fusion, we generated a transgenic mouse line that expressed CD9-EGFP only in eggs (Fig. 1*A*), and converted to the genetic background of $CD9^{-/-}$ mice by mating mice. Western blot analysis using anti-CD9 monoclonal antibody (mAb) revealed that an expected CD9-EGFP with a molecular mass of 51 kDa (CD9 and EGFP contributing to 24 and 27 kDa, respectively) was expressed in the eggs collected from $Tg^+CD9^{-/-}$ mice; however, the amount of CD9-EGFP expressed in $CD9^{-/-}$ eggs was estimated to be 10% of that of endogenous CD9 in the $CD9^{+/+}$ eggs (Fig. 1*B*). Despite the small amount of CD9-EGFP expressed in eggs, CD9-EGFP demonstrated the ability to reverse the sterility of $CD9^{-/-}$ females (Fig. 1*C*). The numbers of pups obtained from $Tg^+CD9^{-/-}$ females (6.4 ± 0.5) were similar to those from

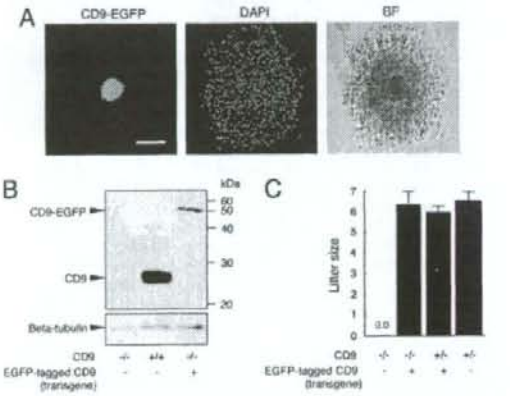

Fig. 1. Generation of mice expressing CD9-EGFP in eggs. (*A*) CD9-EGFP specifically expressed in eggs with mouse ZP3-promoter. Cumulus oocyte complex from $Tg^+CD9^{-/+}$ oviducts was collected at 14 h after injection of human chorionic gonadotropin. Nuclei of an egg and cumulus cells were counterstained with DAPI. (*Left*) CD9-EGFP. (*Center*) DAPI. (*Right*) Bright field. Scale bar: 100 μm. (*B*) Western blot analysis for eggs collected from $CD9^{-/-}$, $CD9^{+/+}$, and $Tg^+CD9^{-/-}$ mice. The same amounts, including 30 eggs of each lysate, were examined by anti-CD9 and anti-beta-tubulin mAbs (internal control). (*C*) Litter sizes of $CD9^{-/-}$ ($n = 31$), $Tg^+CD9^{-/-}$ ($n = 35$), $Tg^+CD9^{+/-}$ ($n = 16$), and $CD9^{+/-}$ mice ($n = 15$) (mean ± SEM). The numbers of females examined are in parentheses.

Author contributions: K. Miyado, K. Yamagata, M.O., and A.U. designed research; K. Miyado, K. Yoshida, K.S., X.W., K. Miyamoto, H.A., T.K., Y.T., T.B., C.I., A.N., M.I., and M.M. performed research; K. Miyado contributed new reagents/analytic tools; K. Miyado, K. Yoshida, H.A., K.T., E.M., and A.U. analyzed data; and K. Miyado wrote the paper.

The authors declare no conflicts of interest.

This article is a PNAS Direct Submission.

Freely available online through the PNAS open access option.

‡K. Miyado and K. Yoshida contributed equally to this work.

§To whom correspondence should be addressed. E-mail: kmiyado@nch.go.jp.

This article contains supporting information online at www.pnas.org/cgi/content/full/0710608105/DCSupplemental.

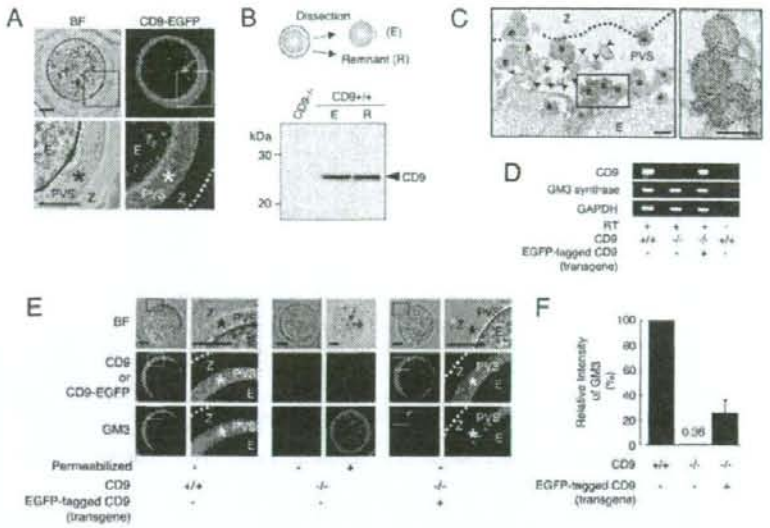

Fig. 2. Identification of secretory vesicles containing CD9 from unfertilized eggs. *A*, A single confocal image showing CD9-EGFP in unfertilized $Tg^+CD9^{-/-}$ eggs (E), including the PVS (*), zona pellucida (Z), and the outer margin of the zona pellucida (dotted line). (*Left*) Bright field. (*Right*) CD9-EGFP. *Lower* are enlarged images of the boxed areas. (*B*) Western blot analysis for eggs mechanically fractionated as shown in the diagram: zona-intact $CD9^{-/-}$ eggs (E) (10 eggs per lane) and zona-free $CD9^{+/+}$ eggs (10 eggs per lane). The medium (R) containing the remnant material from 40 eggs treated with a piezo manipulator was loaded in each lane. (*C*) Immunoelectron-microscopic analysis of $CD9^{+/+}$ eggs. The zona-intact $CD9^{+/+}$ eggs were examined using anti-CD9-mAb and 5-nm gold beads conjugated with anti-rat IgG Ab. Left panel: Image including CD9-containing vesicles (*), microvilli (arrowheads), zona pellucida (Z), perivitelline space (PVS), and egg (E). (*Right*) An enlarged image of the boxed region in the left panel. Scale bar: 200 nm. (*D*) RT-PCR for CD9, GM3 synthase, and glyceraldehyde-3-phosphate dehydrogenase transcripts in $CD9^{+/+}$, $CD9^{-/-}$, and $Tg^+CD9^{-/-}$ eggs. The same amounts, including 50 eggs in each reaction, were examined. The right end lanes are negative controls in which RT was removed from reactions of wild-type eggs. (*E*) Localization of GM3 and CD9 in $CD9^{+/+}$, $CD9^{-/-}$, and $Tg^+CD9^{-/-}$ eggs. (*Left*) Wild-type. (*Middle*) $CD9^{-/-}$. (*Right*) $Tg^+CD9^{-/-}$. Right-side of the sets of wild-type and $Tg^+CD9^{-/-}$ eggs are enlarged images of the boxed regions. The live eggs were examined, and the internal localization of GM3 in $CD9^{-/-}$ eggs was examined under fixed, permeabilized conditions. (*F*) Comparison of the fluorescent intensities of GM3 stained by antibody in wild-type (n = 10), $CD9^{-/-}$ (n = 9), and $Tg^+CD9^{-/-}$ eggs (n = 10) (mean ± SEM). The average values of the wild-type eggs were set to 100%.

$Tg^+CD9^{+/-}$ and $CD9^{+/-}$ females (6.0 ± 0.2 and 6.5 ± 0.5) and greater than those from $CD9^{-/-}$ females (0.0 ± 0.0). The $CD9^{+/-}$ females did not exhibit any loss in fertility that could cause a reduction of litter size relative to that of the $CD9^{+/+}$ females (4). Furthermore, the transgene had no effect on normal fertility. These results demonstrate that transgenically expressed CD9-EGFP can compensate for the loss of intrinsic CD9 and yield eggs with the ability to fuse with sperm.

Based on the foregoing evidence, we observed the subcellular localization of CD9-EGFP in "living" $Tg^+CD9^{-/-}$ eggs (Fig. 2*A*). As expected, confocal microscopic analysis allowed the visualization of two types of CD9-EGFP localization: intense on the plasma membrane and also in the cytoplasm. Unexpectedly, we found loosely filled, noncompacted CD9-EGFP in the PVS, a space formed between the zona pellucida and the plasma membrane of the egg. The localization of CD9 outside the eggs also was confirmed by Western blot analysis using anti-CD9 mAb (Fig. 2*B*). As shown in the diagram, $CD9^{+/+}$ eggs were mechanically fractionated into denuded eggs and other components (R) using a piezo manipulator (11). The fraction R, containing the zona pellucida and the components in the PVS, was centrifuged and subjected to Western blot analysis. The amount of CD9 in the remnant material from 40 eggs was found to be densitometrically equal to that of 10 zona-free eggs, demonstrating an estimated relative abundance of CD9 in the remnant of 20% per egg. Subsequently, we performed immunoelectron-microscopic analysis on the $CD9^{+/+}$ eggs. We identified the vesicles bound to gold particles inside the PVS (Fig. 2*C*). The sectioned microvilli contained a branched network of actin filaments, whereas the variously sized vesicles (50–250 nm in diameter) had uniformly dense materials rather than actin filaments. We also compared $CD9^{+/+}$, $Tg^+CD9^{-/-}$, and $CD9^{-/-}$ eggs by electron-microscopic analysis [supporting information (SI) Fig. S1]. The accumulation of vesicles in the PVS in the $Tg^+CD9^{-/-}$ eggs was comparable to that in the $CD9^{+/+}$ eggs, whereas it was not seen in the $CD9^{-/-}$ or germinal vesicle-staged $CD9^{+/+}$ eggs. These results indicate that 20% of the total amount of CD9 is stored as vesicles in the PVS during meiosis.

We next examined the expression of ganglioside GM3, identified as a CD9-associated molecule (12) and a component of exosomes (10), in $CD9^{+/+}$, $CD9^{-/-}$, and $Tg^+CD9^{-/-}$ eggs. First, we confirmed the expression of GM3 synthase (ST3GalV/SAT-1) (13) in these eggs by RT-PCR (Fig. 2*D*). Then we investigated the localization of GM3 by immunostaining these live eggs with anti-GM3 mAb (Fig. 2*E*). This antibody has been demonstrated to recognize GM3 in the plasma membrane of cells without treatment for permeabilization (14). Finally, we measured the fluorescent intensities of GM3 in these live eggs (Fig. 2*F*). As expected, in wild-type eggs, GM3 was colocalized with CD9 in the PVS and plasma membrane (Fig. 2*E Left* and Fig. 2*F*). In contrast, in $CD9^{-/-}$ eggs, the fluorescent intensities of GM3 were decreased dramatically in the PVS and plasma membrane (0.4% ± 0.2%, relative to 100% for the $CD9^{+/+}$ eggs), consistent with the loss of CD9 (Fig. 2*E Center* and Fig. 2*F*), whereas GM3 could be detected in the cytoplasm of $CD9^{-/-}$ eggs that had been permeabilized by a detergent after fixation. Moreover, the expression of CD9-EGFP reversed the decrease of GM3 in the PVS and plasma membrane of $CD9^{-/-}$ eggs (25.6 ± 10.7%) (Fig. 2*E Right* and Fig. 2*F*), corresponding to the amount of CD9-EGFP quantified by Western blot analysis (Fig. 1*B*). In addition, electron-microscopic analysis revealed that the number of characteristic membrane structures, termed microvilli (1), were significantly decreased in the $CD9^{-/-}$ eggs compared with the $CD9^{+/+}$ eggs (Fig. S2 *A* and *B*). The numbers of microvilli were increased by ≈50% by the expression of CD9-EGFP in the $CD9^{-/-}$ eggs. The analyses of three types of eggs indicate that CD9- and GM3-containing vesicle release is linked to microvilli formation.

We next investigated the involvement of CD9-containing vesicles in sperm–egg fusion (Fig. 3). We found that, based on the length of microvilli (Fig. S2*C*), zona-intact $Tg^+CD9^{-/-}$ eggs can be categorized into two groups (Fig. 3*A*). From single

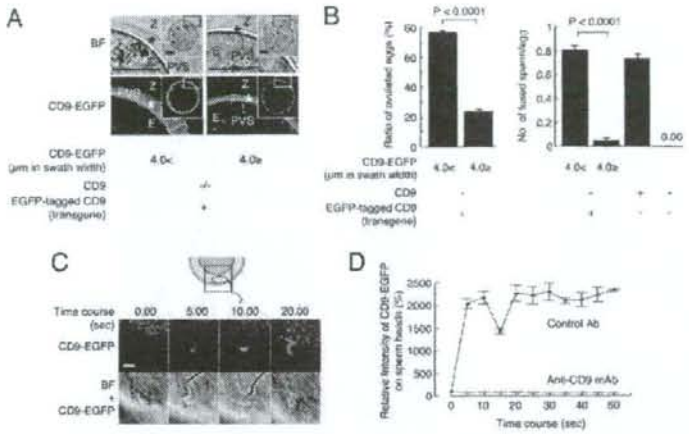

Fig. 3. Involvement of CD9-containing vesicles in sperm–egg fusion. (*A*) Categorization of $Tg^+CD9^{-/-}$ eggs (E) into two groups according to the thickness of CD9-EGFP in the PVS (*) and the inner region of the zona pellucida (Z) (>4.0 μm or ≤ 4.0 μm), indicated by double-headed lines. The boxed regions in *Insets* are enlarged. Scale bar: 20 μm. (*B*) Comparison of the fusing ability of two groups of $Tg^+CD9^{-/-}$ eggs with wild-type sperm. Left graph: Ratio of two groups of $Tg^+CD9^{-/-}$ eggs ovulated from 12 females (mean ± SEM). Right graph: Number of sperm fused per egg in two groups of zona-intact $Tg^+CD9^{-/-}$ eggs ovulated from 12 females (>4.0 μm, $n = 204$; ≤4.0 μm, $n = 66$) (mean ± SEM). $CD9^{+/+}$ ($n = 120$) and $CD9^{-/-}$ ($n = 112$) served as positive and negative controls, respectively. (*C* and *D*) Monitoring of the association of egg CD9-containing vesicles with wild-type sperm. $Tg^+CD9^{-/-}$ eggs were incubated with the sperm and monitored immediately after the sperm penetrated the zona pellucida under the presence of anti-CD9 mAb (boxed region). The values were calculated from data scanning by confocal microscopy (15 sperm in triplicate dishes) Blue: Preimmune rat IgG. Red: Anti-CD9 mAb (KMC8) (mean ± SEM). The average values of the fluorescent intensities of CD9-EGFP at 0 s were set to 100%, and the final concentration of antibodies was adjusted to 50 μg/ml. Scale bar, 5 μm.

confocal images sectioned through the largest diameter, the accumulation of CD9-EGFP from the plasma membrane to the inner region of the zona pellucida was >4.0 μm in swath width in one group and ≤ 4.0 μm in the other group. The accumulation of CD9-EGFP was predicted to show that CD9-containing vesicles are more highly accumulated within the PVS in the >4.0-μm group compared with the ≤ 4.0-μm group. Comparing the ratio of these two groups in $Tg^+CD9^{-/-}$-ovulated eggs revealed a much higher percentage of the >4.0-μm group (77.0 ± 1.3% vs.23.7 ± 1.5%) (Fig. 3*B Left*). Therefore, we focused on the heterogeneity of CD9-EGFP accumulation within the PVS and determined the ratio of the two groups in zona-intact $Tg^+CD9^{-/-}$ eggs that successfully fused with the sperm 6 h after insemination. The >4.0-μm group of $Tg^+CD9^{-/-}$ eggs showed higher activity for fusion with sperm (0.81 ± 0.04 sperm fused per egg), compared with the ≤40-μm group of $Tg^+CD9^{-/-}$ eggs (0.05 ± 0.03) and the $CD9^{-/-}$ eggs (0.00 ± 0.00), and comparable activity to that of wild-type eggs (0.73 ± 0.04) (Fig. 3*B Right*). The average activity of all $Tg^+CD9^{-/-}$ eggs (0.72 ± 0.03 sperm fused per egg) was equal to that of wild-type eggs (0.73 ± 0.04 sperm fused per egg). The difference between the two groups of $Tg^+CD9^{-/-}$ eggs was statistically significant (Fig. 3*B*). These results suggest that the quantities of CD9-containing vesicles, as assessed by the swath width of CD9-EGFP, are strongly correlated with the frequency of sperm–egg fusion.

To detect the association between sperm and CD9-containing vesicles, we serially monitored the wild-type sperm that penetrated the zona pellucida of the $Tg^+CD9^{-/-}$ eggs (Fig. 3 *C* and *D*). As shown in the diagram, we began monitoring the sperm immediately after the head portion of sperm penetrated the zona pellucida of the $Tg^+CD9^{-/-}$ eggs (Fig. 3*C Upper*, boxed area in the diagram). Soon after we began to monitor the sperm, the fluorescent intensities of CD9-EGFP on the sperm heads increased and then decreased rapidly between 0 s and 15 s, then increased again, reaching a maximum at 20 s. At this point, the CD9-EGFP fully covered the surface of the sperm heads. In contrast, when the sperm were incubated with $Tg^+CD9^{-/-}$ eggs in the medium containing anti-CD9 mAb, no increase in intensity of CD9-EGFP on the sperm heads was detected. Anti-CD9 mAbs have been reported to inhibit sperm–egg fusion (4, 15, 16). Our findings demonstrate that the anti-CD9 mAb inhibited the association of sperm with CD9-containing vesicles in parallel to inhibition of sperm–egg fusion.

To determine whether CD9-containing vesicles are capable of initiating sperm–egg fusion, we incubated the sperm with $CD9^{-/-}$ eggs in medium containing the vesicles collected from $CD9^{+/+}$ eggs (Fig. 4 and Fig. S3). To restrict the source of CD9 into the vesicles from the $CD9^{+/+}$ eggs, we used sperm collected from the epididymis of $CD9^{-/-}$ males. We estimated the capability of the vesicles to influence fusion by counting the number of sperm fused with $CD9^{-/-}$ eggs. As shown in the experimental design, after the zona pellucida was removed from the $CD9^{-/-}$ eggs, the eggs were incubated with sperm in the medium containing the vesicles (Fig. 4*A*). When examined at 1 h after incubation, the sperm were seen to be capable of fusing with $CD9^{-/-}$ eggs after co-incubation with the vesicles (Fig. 4*A Center*), indicating restoration of the fusibility of $CD9^{-/-}$ eggs with the sperm (0.58 ± 0.07 sperm fused per egg) (Fig. 4*B*). We detected further evidence of sperm–egg fusion in the $CD9^{-/-}$ eggs from which a second polar body had been extruded. In contrast, we did not detect improved fusibility of sperm with eggs in medium depleted of CD9-containing vesicles using beads conjugated with anti-CD9 mAb (Fig. 4*A Right* and *B*). After treatment with the beads, the quantity of CD9 in the depleted medium was significantly decreased, to 16% of the untreated medium (Fig. 4*C*). In addition, $CD9^{-/-}$ remnants failed to rescue the fusing ability of $CD9^{-/-}$ eggs. These findings indicate that the association with CD9-containing vesicles renders the sperm capable of fusing with eggs without endogenous CD9 expression. We estimated the relative abundance of CD9 in the remnant as 18% of the total amount in the eggs (Fig. 4*C*). We further found

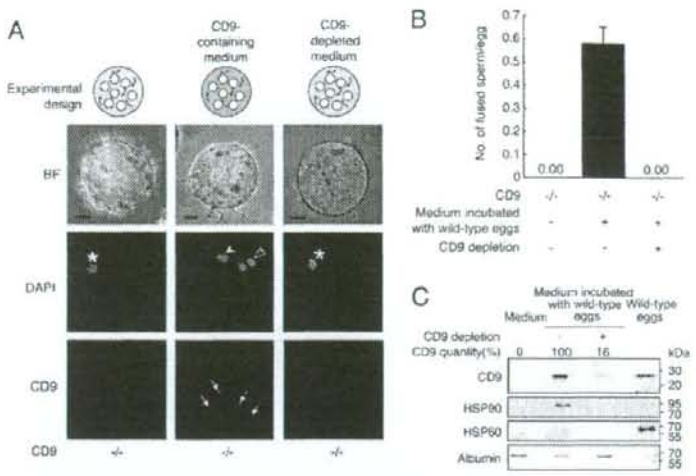

Fig. 4. Identification of fusion-facilitating activity of CD9-containing vesicles. (*A*) Estimation of the fusion-facilitating ability of the vesicles in sperm–egg fusion. As shown in the experimental design, $CD9^{-/-}$ sperm were incubated with $CD9^{-/-}$ eggs (white circles) in media containing egg-released vesicles after the zona pellucida was removed from these eggs. CD9 was detected by anti-CD9 mAb conjugated with Alexa488. The eggs were preloaded with DAPI before incubation with the sperm, to allow counting of the number of fused sperm. (*Left*) $CD9^{-/-}$ eggs at 1 h after incubation with the sperm, as a negative control. *Center* $CD9^{-/-}$ eggs cultured in the medium containing CD9 collected from wild-type eggs. (*Right*) $CD9^{-/-}$ eggs cultured in the medium depleted of CD9 by beads conjugated with anti-CD9 mAb, showing the fused sperm to eggs (arrowhead), metaphase II–arrested chromosomes (*), a second polar body (open arrowhead), and CD9 translocated on the sperm heads (arrow). The fluorescent z-series images were projected as three-dimensional images. Scale bar: 20 μm. (*B*) Number of fused sperm with the zona-free eggs counted at 1 h after incubation (mean ± SEM): $CD9^{-/-}$ eggs as a negative control (n = 51), $CD9^{-/-}$ eggs cultured in the medium containing CD9 (n = 112), and $CD9^{-/-}$ eggs cultured in the medium depleted of CD9 by antibody-conjugated beads (n = 74). The total numbers of eggs examined are in parentheses. (*C*) Western blot analysis of the media incubated with $CD9^{+/+}$ eggs for CD9, HSP90, and HSP60. Loaded samples (left to right): The medium as a negative control, the medium containing the remnant material from 40 eggs per lane (bead-untreated and -treated), and 5 eggs per lane as a positive control. The albumin contained in the medium was detected by Coomassie brilliant blue staining as an internal control. The quantities of CD9 in the media were measured densitometrically (using National Institutes of Health Image software).

that the decreased amount of CD9 after the bead treatment was synchronized with that of a cytoplasmic chaperone, HSP90 (17), but not with a mitochondrial chaperone, HSP60 (18). Our analysis of the egg-conditioned medium indicated that CD9-containing vesicles contained HSP90, a conserved component of exosomes (9, 10).

To estimate the contribution of CD9-containing vesicles to sperm–egg fusion, we examined the restoration of the impaired sperm-fusing ability in $CD9^{-/-}$ eggs co-incubated with $CD9^{+/-}$ or $CD9^{+/+}$ eggs expressing endogenous CD9 (Figs. 5 and S4*A*). We predicted that when sperm were incubated with a mixture of eggs, the vesicles released from $CD9^{+/-}$ or $CD9^{+/+}$ eggs would

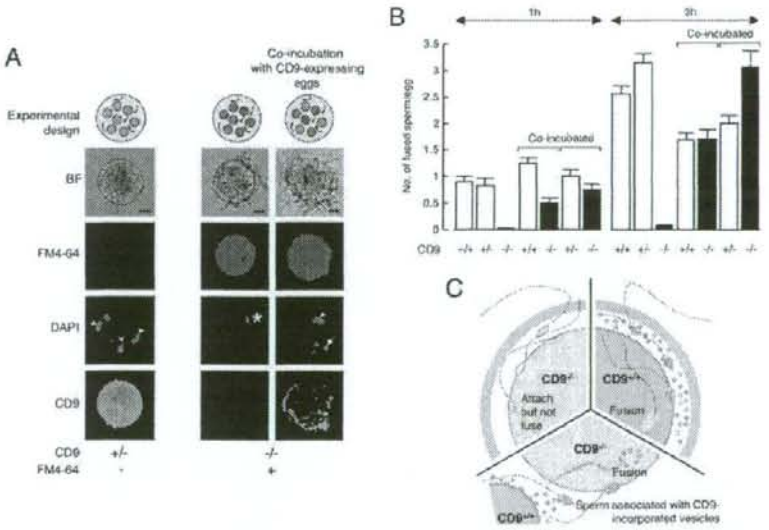

Fig. 5. Recovery of impaired fusion of $CD9^{-/-}$ eggs with sperm by CD9-containing vesicles. (*A*) Estimation of the fusion-facilitating ability of the vesicles in sperm–egg fusion. As shown in the experimental design, sperm were incubated with a mixture of CD9-expressing eggs (green circles) and $CD9^{-/-}$ eggs (red circles) after the zona pellucida was removed from these eggs. The eggs were preloaded with DAPI before incubation with sperm, to allow counting of the number of fused sperm. $CD9^{-/-}$ eggs were prestained with FM4–64 and thus were easily distinguished from CD9-expressing eggs after incubation with the sperm. (*Left*) $CD9^{+/-}$ eggs at 1 h after incubation with the sperm, as a positive control. (*Center*) $CD9^{-/-}$ eggs, as a negative control. (*Right*) $CD9^{-/-}$ eggs co-incubated with $CD9^{+/-}$ eggs, showing fused sperm to egg (arrowheads), metaphase II–arrested chromosomes (*), and extruded second polar body (arrow). The fluorescent z-series images were projected as three-dimensional images. CD9 was detected by anti-CD9 mAb conjugated with Alexa488. Scale bar: 20 μm. (*B*) Numbers of fused sperm with the zona-free eggs counted at 1 and 3 h after incubation (mean ± SEM). $CD9^{+/-}$ (1 h: n = 34; 3 h: n = 55), $CD9^{+/+}$ (1 h: n = 71; 3 h: n = 79), and $CD9^{-/-}$ eggs (1 h: n = 100; 3 h: n = 115) were separately incubated with sperm. Total number of coincubated eggs examined: $CD9^{+/-}$ eggs (n = 54) coincubated with $CD9^{-/-}$ eggs (n = 60), and $CD9^{+/+}$ eggs (n = 65) coincubated with $CD9^{-/-}$ eggs (n = 74) at 1 h; $CD9^{+/-}$ eggs (n = 51) coincubated with $CD9^{-/-}$ eggs (n = 33), and $CD9^{+/+}$ eggs (n = 98) coincubated with $CD9^{-/-}$ eggs (n = 90) at 3 h. (*C*) Schematic model of involvement of CD9-containing vesicles in sperm–egg fusion: $CD9^{+/+}$ (green), $CD9^{-/-}$ (light blue), and $CD9^{-/-}$ eggs coincubated with $CD9^{+/+}$ wild-type eggs with sperm (yellow).

interact with sperm, and these sperm could fuse with $CD9^{-/-}$ eggs. If sperm-fusing ability were regulated mainly by CD9-containing vesicles, then the number of sperm fused to $CD9^{-/-}$ eggs would be predicted to be almost equal to that fused to $CD9^{+/-}$ or $CD9^{+/+}$ eggs coincubated with $CD9^{-/-}$ eggs. We counted the number of fused sperm in coincubated CD9-expressing eggs ($CD9^{+/-}$ and $CD9^{+/+}$) and $CD9^{-/-}$ eggs. The $CD9^{-/-}$ eggs were prestained with FM4–64 (19), a fluorescent dye used to stain the membrane of live cells, and thus could be easily distinguished from the $CD9^{+/-}$ and $CD9^{+/+}$ eggs. FM4–64 did not transfer between the $CD9^{-/-}$ eggs and the $CD9^{+/-}$ or $CD9^{+/+}$ eggs. As shown in the experimental design, after the zona pellucida was removed from the eggs, $CD9^{-/-}$ eggs (red circles) were mixed with $CD9^{+/-}$ or $CD9^{+/+}$ eggs (green circles), and sperm were added to the medium containing these eggs (Fig. 5*A*). At 1 h after insemination, significant fusion of sperm with the $CD9^{-/-}$ eggs was facilitated (0.75 ± 0.11 and 0.50 ± 0.09 sperm fused per egg), corresponding to that in the $CD9^{+/-}$ (1.00 ± 0.13) and $CD9^{+/+}$ eggs (1.25 ± 0.10). At 3 h after insemination, the fusion of sperm with the $CD9^{-/-}$ eggs was restored (3.06 ± 0.30 and 1.70 ± 0.18 sperm fused per egg) to levels comparable to those in the $CD9^{+/-}$ (2.00 ± 0.15) and $CD9^{+/+}$ eggs (1.69 ± 0.13). We also detected a second polar body extruding from the $CD9^{-/-}$ eggs (Fig. 5*A Right*, arrow). In contrast, we did not observe the translocation of vesicles from the $CD9^{+/-}$ and $CD9^{+/+}$ eggs to the $CD9^{-/-}$ eggs when sperm were not added to the mixture, even after 10 h of incubation (Fig. S4*B*). These data demonstrate that the defect in the fusing ability of $CD9^{-/-}$ eggs is caused by dysfunction of the mechanism facilitating the sperm-fusing activity through CD9-containing vesicles.

To further study the involvement of CD9-containing vesicles in regulating sperm-fusing ability, we evaluated the capability of hamster eggs in sperm–egg fusion (Fig. S5). Hamster eggs have the ability to fuse with other mammalian sperm and thus are used as a tool to evaluate the fusing ability of human sperm (20). When hamster eggs were incubated with $CD9^{-/-}$ eggs after the zona pellucida was removed from these eggs, the sperm-fusing ability of these eggs was improved significantly. The sperm-fusing ability acquired through the exposure to hamster eggs was not as great as that produced by exposure to mouse eggs, probably due to the slightly different CD9 in hamster and mouse eggs (21). These results indicate that the function of CD9-containing vesicles in the acquisition of sperm-fusing ability is widely conserved in mammals.

Discussion

In sperm–egg fusion, there is a significant direct interaction between the cell membranes of sperm and eggs (1, 20, 22); however, our results demonstrate that CD9-containing vesicle–sperm interaction precedes the direct cell membrane interaction between sperm and eggs. Based on our data, we propose that the release of CD9-containing vesicles from eggs before fertilization facilitates the sperm-fusing ability that renders the sperm competent to fuse with $CD9^{-/-}$ eggs (Fig. 5*C*). Our finding of CD9-EGFP in living unfertilized eggs demonstrates that CD9-containing vesicles are present in the PVS, and that these vesicles accumulate inside the PVS during the germinal vesicle (1) and metaphase II-arrested stages (1). During this period, the egg undergoes drastic cytological changes with the increased number of microvilli (1, 22), predicting the correlation between vesicle release and microvilli formation. As expected, this correlation is supported by the finding that CD9 deficiency leads not only to impaired microvilli formation (8) (Fig. S2), but also to decreased accumulation of vesicles within the PVS. These data support the association between the release of CD9-containing vesicles from eggs and the formation of microvilli on the egg plasma membrane.

As reported previously, somatic cells are capable of releasing proteins and lipids included in membrane organelles, termed exosomes (9, 10), which are pinched out from the plasma membrane (23). Exosomes share many additional properties with retroviral particles, including similar lipid and protein compositions, such as tetraspanin (23). GM3 and HSP90 are known to be conserved components of exosomes (10). Our results show that CD9-containing vesicles released from eggs share these two components, implying that the vesicles are "exosome-like." Previous studies of macrophages have proposed that exosome biogenesis occurs only by outward budding at endosomal membranes, followed by the fusion of vesicle-laden endosomes with the plasma membrane (9, 23). If the CD9-containing vesicle were derived from exosomes and generated from the fusion of endosomes with the plasma membrane, then the vesicles would contain some proteases (9, 23), fuse with the sperm membrane, and possibly activate the sperm fusogenic factor(s) by enzymatic activities.

In hamster eggs, expansion of the PVS has been deemed essential or at least beneficial to normal fertilization (20, 21, 24), indicating that materials involved in fusion with sperm are released from eggs before fertilization in hamsters and in mice. Because anti-CD9 mAbs are not available for hamster CD9, we could not directly confirm CD9-containing vesicle release from hamster eggs before fertilization. Instead, our co-incubation assay demonstrated that hamster eggs facilitate the fusion of sperm with $CD9^{-/-}$ eggs, indicating that hamster eggs share a similar mechanism with mouse eggs through egg-released materials. Moreover, it has been reported that growing oocytes bind to sperm and transfer fluorescent dyes to the sperm head (25). At this stage, oocytes have CD9 on the cell membrane but lack CD9-containing vesicles (Fig. S1). We presume that the transfer of fluorescent dye from growing oocytes to sperm heads is mediated by CD9 on the cell membrane. Based on our findings, we propose that the CD9-containing vesicle has an ability to facilitate sperm—egg fusion. This knowledge has great potential for clinical applications, such as the induction of sperm–egg fusion using exogenous sources.

Materials and Methods

Animals. The mice that we produced were back-crossed into a C57BL/6 genetic background. Wild-type eggs were collected from C57BL/6 females (8–12 weeks old). Wild-type sperm were obtained from the epididymides of B6C3F1 males (8–12 weeks old). Hamster eggs were obtained commercially as frozen unfertilized eggs (NOSAN).

Antibodies and Chemicals. Antibodies against CD9 (KMC; BD PharMingen), beta-tubulin (Tub2.1; Sigma), HSP60 (24/HSP60; BD PharMingen), HSP90 (16F1; MBL), and GM3 (GMR6; Seikagaku) were used. Antibodies labeled with biotin by a labeling kit (Dojindo) and horseradish peroxidase-conjugated streptavidin (Sigma) were used for Western blot analysis. For immunostaining, antibodies were labeled directly with Alexa488 and Alexa546 using labeling kits (Invitrogen). FM4–64 (Invitrogen) was used to define the lipid bilayer of live eggs without disturbing sperm–egg fusion (10 μM at final concentration). We used DAPI (Invitrogen), a fluorescent dye that slowly permeates the living cell membrane (semipermeable) and slowly leaks out of cells after washing relative to Hoechst33342 (permeable), in counting the number of sperm fused per egg.

Transgenic Mice. The construct expressing mouse CD9 tagged at the N terminus with EGFP (CD9-EGFP) was subcloned into plasmid DNA-containing mouse ZP3 promoter (26). The expression cassette was excised by restriction enzyme digestion and microinjected into fertilized eggs of C57BL/6 mice, according to standard techniques (27).

Genotyping and RT-PCR. Mouse genotyping and RT-PCR were performed following standard procedures (27). (Primer sets are listed in Table S1).

Egg Collection. Eggs were collected from the oviduct 14–16 h after human chorionic gonadotropin injection (4). The eggs were placed in a drop of TYH

medium (28). Sperm collected from the epididymides were capacitated in a 100-μl drop of medium. The eggs were incubated with 1.5×10^5 sperm/ml at 37°C in 5% CO_2, and unbound sperm were washed away. The zona pellucida was removed from the eggs with acidic Tyrode's solution (4) or a piezo manipulator (11). A hole was punched through the zona pellucida with a piezo manipulator, and the eggs were removed. All materials were aspirated, including the medium but not the eggs, and used as "remnants."

Immunostaining. Zona-intact live eggs were stained with diluted antibodies in TYH medium for 30 min at 37°C, and the nonspecifically accumulated antibodies in the PVS were washed away after a brief incubation (30 min) in the medium. To measure the fluorescent intensities of GM3, three types of eggs were stained by AlexaS46-labeled anti-GM3 mAb in TYH medium for 30 min, then washed in the medium for 30 min. Staining was visualized using a laser scanning confocal microscope (LSM 510 META; Carl Zeiss).

Electron-Microscopic Analysis. Live eggs were incubated with anti-CD9 mAb and anti-rat IgG mAb tagged with 5-nm gold beads. After incubation, the eggs were fixed by glutaraldehyde and osmic acid solutions. Ultra-thin sections were prepared as described in ref. 29. Eggs denuded with acid Tyrode's solution were fixed with a mixture of paraformaldehyde and glutaraldehyde and osmic acid solutions.

***In Vitro* Fertilization.** To observe the fusion with the sperm, zona-intact and zona-free eggs were incubated with DAPI (10 μg/ml) in the medium for 20 min, then washed before the sperm were added. This procedure allowed the staining of only fused sperm nuclei by dye-transfer into sperm after membrane fusion. At 1 h or 3 h after incubation in a 30-μl drop of medium, the eggs were fixed with a mixture of paraformaldehyde and glutaraldehyde for 20 min at 4°C.

Monitoring the Association of CD9-Containing Vesicles with Sperm. Eggs collected from $Tg^+CD9^{-/-}$ females were set in a 30-μl drop of TYM medium. The sperm were added to the eggs at a final concentration of 1.5×10^5/ml after incubation in the medium for 2 h. Posts of latex beads were deposited around the eggs. A glass coverslip was carefully pressed down onto the posts until the egg were fixed. The medium containing eggs and sperm was cooled to 10°C before observation. Cooling reduced the sperm motility. This procedure allowed us to measure the CD9-EGFP fluorescence on the sperm head using a confocal microscope. Images of the sperm were captured at 1 frame/s. The average value of the fluorescent intensities of CD9-EGFP at 0 s was set to 100%, and the final concentration of antibodies was adjusted to 50 μg/ml. The data are measurements of serial images from 15 wild-type sperm in triplicate dishes.

Collection of CD9-Containing Vesicles. The medium containing the vesicles was collected from denuded wild-type eggs. The eggs were cultured in a 60-μl drop of medium for 2 h after the zona pellucida was removed from the eggs. Collecting the medium containing the vesicles required an incubation time of 2 h. The collected medium was used for analysis of vesicle components and evaluation of sperm-fusing ability. CD9-depleted medium was used as a negative control. After the zona pellucida was removed from $CD9^{-/-}$ eggs, the eggs were incubated with the sperm in the medium containing CD9-incorporated vesicles for 1 h, for comparison with the vesicle-depleted medium. Details are shown in Fig. S3.

Western Blot Analysis. Quantities of proteins were examined by Western blot analysis, as described in ref. 4. As an internal loading control, quantities of albumin included in the medium were examined using Coomassie brilliant blue staining. Details are shown in Fig. S3.

Coincubation of Two Types of Eggs. $CD9^{-/-}$ eggs and CD9-expressing eggs ($CD9^{+/-}$ and $CD9^{+/+}$) were incubated in each 30-μl drop of medium after the zona pellucida was removed from these eggs. At 2 h after incubation, the $CD9^{-/-}$ eggs were added into the cultured medium of the CD9-expressing eggs. Sperm were added into the medium containing two types of eggs and incubated for 1 or 3 h. Details are shown in Fig. S4A. The frozen hamster eggs also were incubated with the $CD9^{-/-}$ eggs and wild-type sperm for 1 h. The zona pellucida of frozen hamster eggs was hardened, and removing the zona pellucida using acid Tyrode's solution took 5 min. Details are shown in Fig. S5A.

ACKNOWLEDGMENTS. This work was supported by a Precursory Research for Embryonic Science and Technology (PRESTO) grant from the Japanese Ministry of Health, Labor and Welfare and by a Grant-in-Aid for Scientific Research from the Japanese Ministry of Education, Culture, Sports, and Technology.

1. Yanagimachi R (1994) in *The Physiology of Reproduction*, eds Knobil E, Neill JD (Raven, New York), pp 189–317.
2. Kaji K, *et al.* (2000) The gamete fusion process is defective in eggs of Cd9-deficient mice. *Nat Genet* 24:279–282.
3. Le Naour F, Rubinstein E, Jasmin C, Prenant M, Boucheix C (2000) Severely reduced female fertility in CD9-deficient mice. *Science* 287:319–321.
4. Miyado K, *et al.* (2000) Requirement of CD9 on the egg plasma membrane for fertilization. *Science* 287:321–324.
5. Hemler ME (2003) Tetraspanin proteins mediate cellular penetration, invasion, and fusion events and define a novel type of membrane microdomain. *Annu Rev Cell Dev Biol* 19:397–422.
6. Barraud-Lange V, Naud-Barriant N, Bomsel M, Wolf J-P, Ziyyat A (2007) Transfer of oocyte membrane fragments to fertilizing spermatozoa. *FASEB J* 21:3446–3449.
7. Joly E, Hudrisier D (2003) What is trogocytosis and what is its purpose? *Nat Immunol* 4:815.
8. Runge K-E, *et al.* (2007) Oocyte CD9 is enriched on the microvillar membrane and required for normal microvillar shape and distribution. *Dev Biol* 304:317–325.
9. Trajkovic K, *et al.* (2008) Ceramide triggers budding of exosome vesicles into multivesicular endosomes. *Science* 319:1244–1247.
10. Wubbolts R, *et al.* (2003) Proteomic and biochemical analyses of human B cell-derived exosomes: Potential implications for their function and multivesicular body formation. *J Biol Chem* 278:10963–10972.
11. Yamagata K, *et al.* (2002) Sperm from the calmegin-deficient mouse have normal abilities for binding and fusion to the egg plasma membrane. *Dev Biol* 250:348–357.
12. Mitsuzuka K, Handa K, Satoh M, Arai Y, Hakomori S (2005) A specific microdomain ("glycosynapse 3") controls phenotypic conversion and reversion of bladder cancer cells through GM3-mediated interaction of alpha3beta1 integrin with CD9. *J Biol Chem* 280:35545–35553.
13. Yamashita T, *et al.* (2003) Enhanced insulin sensitivity in mice lacking ganglioside GM3. *Proc Natl Acad Sci USA* 100:3445–3449.
14. Kotani M, Ozawa H, Kawashima I, Ando S, Tai T (1992) Generation of one set of monoclonal antibodies specific for a-pathway ganglio-series gangliosides. *Biochim Biophys Acta* 1117:97–103.
15. Chen MS, *et al.* (1999) Role of the integrin-associated protein CD9 in binding between sperm ADAM 2 and the egg integrin alpha6beta1: Implications for murine fertilization. *Proc Natl Acad Sci USA* 96:11830–11835.
16. Miller B-J, Georges-Labouesse E, Primakoff P, Myles D-G (2000) Normal fertilization occurs with eggs lacking the integrin alpha6beta1 and is CD9-dependent. *J Cell Biol* 149:1289–1296.
17. Callahan M-K, Garg M, Srivastava P-K (2008) Heat-shock protein 90 associates with N-terminal extended peptides and is required for direct and indirect antigen presentation. *Proc Natl Acad Sci USA* 105:1662–1667.
18. Cheng M-Y, Hartl F-U, Horwich A-L (1990) The mitochondrial chaperonin hsp60 is required for its own assembly. *Nature* 348:455–458.
19. Bolte S, *et al.* (2004) FM-dyes as experimental probes for dissecting vesicle trafficking in living plant cells. *J Microsc* 214:159–173.
20. Yanagimachi R, Yanagimachi H, Rogers B-J (1976) The use of zona-free animal ova as a test system for the assessment of the fertilizing capacity of human spermatozoa. *Biol Reprod* 15:471–476.
21. Ponce R-H, Yanagimachi R, Urch U-A, Yamagata T, Ito M (1993) Retention of hamster oolemma fusibility with spermatozoa after various enzyme treatments: A search for the molecules involved in sperm–egg fusion. *Zygote* 1:163–171.
22. Primakoff P, Myles D-G (2002) Penetration, adhesion, and fusion in mammalian sperm–egg interaction. *Science* 296:2183–2185.
23. Booth A-M, *et al.* (2006) Exosomes and HIV Gag bud from endosome-like domains of the T cell plasma membrane. *J Cell Biol* 172:923–935.
24. Okada A, Yanagimachi R, Yanagimachi H (1986) Development of a cortical granule-free area of cortex and the perivitelline space in the hamster oocyte during maturation and following ovulation. *J Submicrosc Cytol* 18:233–247.
25. Zuccotti M, Yanagimachi R, Yanagimachi H (1991) The ability of hamster oolemma to fuse with spermatozoa: Its acquisition during oogenesis and loss after fertilization. *Development* 112:143–152.
26. Rankin T-L, *et al.* (1998) Human ZP3 restores fertility in Zp3 null mice without affecting order-specific sperm binding. *Development* 125:2415–2424.
27. Hogan B, Costantini F, Lacy E (1986) in *Manipulating the Mouse Embryo* (Cold Spring Harbor Lab Press, Cold Spring Harbor, NY), pp 217–252.
28. Toyoda Y, Chang M-C (1974) Capacitation of epididymal spermatozoa in a medium with high K-Na ratio and cyclic AMP for the fertilization of rat eggs in vitro. *J Reprod Fertil* 36:125–134.
29. Toshimori K, Saxena D-K, Tanii I, Yoshinaga K (1998) An MN9 antigenic molecule, equatorin, is required for successful sperm–oocyte fusion in mice. *Biol Reprod* 59:22–29.

Conjoined twins in a triplet pregnancy after intracytoplasmic sperm injection and blastocyst transfer: case report and review of the literature

Tetsuya Hirata, M.D., Ph.D, Yutaka Osuga, M.D., Ph.D, Akihisa Fujimoto, M.D., Ph.D, Hajime Oishi, M.D., Ph.D, Hisahiko Hiroi, M.D., Ph.D, Toshihiro Fujiwara, M.D., Ph.D, Tetsu Yano, M.D., Ph.D, and Yuji Taketani, M.D., Ph.D.

Department of Obstetrics and Gynecology, Faculty of Medicine, University of Tokyo, Tokyo, Japan

Objective: To describe an exceptional case of conjoined twins in a triplet pregnancy after intracytoplasmic sperm injection (ICSI) and blastocyst transfer.
Design: Case report.
Setting: University teaching hospital reproductive endocrinology department and infertility practice.
Patient(s): A 34-year-old woman underwent ICSI and received two blastocysts transferred.
Intervention(s): Transvaginal ultrasonography performed sequentially during early pregnancy.
Main Outcome Measure(s): Ultrasound images of the fetus in gestational sac.
Result(s): Two gestational sacs in the uterus were revealed at the 5th week. At the 8th week of gestation, a single fetus was seen in one sac, whereas thoracopagus conjoined twins was diagnosed in the other sac. At the 10th week, the conjoined twins had a spontaneous cardiac arrest confirmed by color Doppler. The subsequent course was uneventful, and a healthy child was born at 39th week.
Conclusion(s): To date, a small number of cases of conjoined twins in IVF/ICSI pregnancies have been reported, in which most cases were treated with manipulations causing possible trauma in the zona pellucida. Our case is unique in that the transferred embryos were blastocysts that might have had additional damage on the zona pellucida from the longer culture. (Fertil Steril® 2008;■:■–■. ©2008 by American Society for Reproductive Medicine.)

Key Words: Conjoined twins, triplet pregnancy, ICSI, blastocyst transfer, ultrasound

Conjoined twins (CT) are identical twins whose bodies are joined in utero. It is a rare phenomenon, estimated to range from 1 in 200,000 to 1 in 100,000 live births (1). Although the precise etiology of the disease remains to be elucidated, CT result from an abnormal process during the development of monozygotic twins (MZT) and make up about 1% of MZT (2).

As assisted reproduction technologies (ART) have become widely used all over the world to treat infertility, several kinds of techniques to micromanipulate the embryo have been developed. Blastocyst transfer is a technique that can simultaneously maintain high pregnancy rates and prevent higher-order multiple gestation by limiting the number of embryos to transfer (3). However, several reports show that blastocyst transfer is related to a higher incidence of MZT (4–6), implying that the procedure might also enhance the frequency of CT.

In the present report, we present a case of CT in a triplet pregnancy conceived after intracytoplasmic sperm injection (ICSI) and subsequent blastocyst transfer into the uterus. We also reviewed the literature reporting the cases of CT after ART procedure.

Received June 13, 2008; revised July 2, 2008; accepted July 9, 2008.
T.H. has nothing to disclose. Y.O. has nothing to disclose. A.F. has nothing to disclose. H.O. has nothing to disclose. H.H. has nothing to disclose. T.F. has nothing to disclose. T.Y. has nothing to disclose. Y.T. has nothing to disclose.
Reprint requests: Yutaka Osuga, Department of Obstetrics and Gynecology, Faculty of Medicine, University of Tokyo, 7-3-1, Hongo, Bunkyo-ku, Tokyo, 113-8655, Japan (FAX: +81-3-3816-2017; E-mail: yutakaos-tky@umin.ac.jp).

CASE REPORT

A 34-year-old gravida 1 para 1 woman underwent ovulation induction followed by ICSI and embryo replacement. Her husband's sperm analysis showed asthenozoospermia. Her previous pregnancy was achieved by ICSI and day 3 embro transfer (ET). A healthy baby was delivered vaginally at the 37th week of gestation. Her family history and past medical history were unremarkable.

Before starting ovulation induction, pituitary down-regulation was achieved by daily use of a GnRH agonist (nafarelin acetate; Nasanyl; Astellas, Tokyo, Japan) administered at the midluteal phase of the previous cycle (day 9 after ovulation). At day 14 after ovulation, menstruation was confirmed. Then, ovulation induction was performed by daily injections of hMG (Humegon; Organon Japan, Tokyo, Japan) starting on day 5 of the menstrual cycle. After 14 days of the gonadotropin administration (total 1,500 IU), oocyte maturation was triggered by injecting 10,000 IU hCG (Mochida Pharmaceutical Co., Osaka, Japan). At that time, the serum E_2 level was 1,793.3 pg/mL.

Transvaginal oocyte retrieval was performed under sonographic guidance 34 h after hCG administration. Twenty-one

0015-0282/08/$34.00 Fertility and Sterility® Vol. ■, No. ■, ■ 2008 1.e1
doi:10.1016/j.fertnstert.2008.07.1730

FIGURE 1

Microscopic view of the blastocysts transferred: early blastocyst and 4BB by Gardner's blastocyst evaluation criteria.

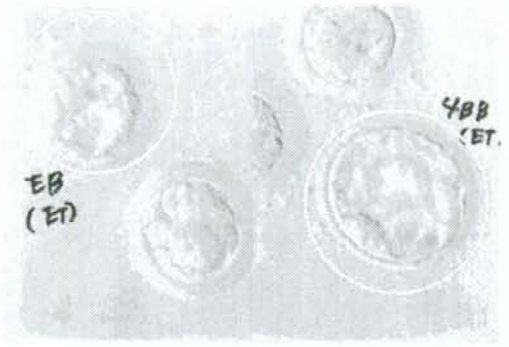

Hirata. Conjoined twins after ART. Fertil Steril 2008.

oocytes were retrieved. Fifteen oocytes were mature (metaphase II) and considered to be suitable for insemination by the ICSI procedure. Thirteen oocytes were fertilized and incubated in cleavage medium (IVC-two; In Vitro Care, San Diego, CA) with 10% human serum albumin. From day 3 after ICSI, all embryos were cultured in sequential media (Sydney IVF Blast Medium; Cook, Brisbane, Australia). Two blastocysts (early blastocyst and 4BB by Gardner's blastocyst evaluation criteria (7)) were obtained and transferred to the uterus on day 5 (Fig. 1). Luteal support was given by administration of 1.44 mg transdermal E_2 patch (Estraderm M; Novartis, Basel, Switzerland) every other day and transvaginal suppository of 200 mg P every day.

Nine days after ET, serum hCG level was 285.0 mIU/mL. At 5 weeks and 3 days of gestation, transvaginal sonography revealed two gestational sacs in the uterus. Transvaginal sonography was thereafter performed at weekly intervals. At 6 weeks 5 days of gestation, a single fetal heartbeat was detected in each of the gestational sac. At the 8th week of gestation, a fetus, with a crown-rump length of 13.5 mm, was seen in one sac, and inseparable fetal bodies were seen in the other sac (Fig. 2). The two fetuses had two separate skulls and were joined at the thorax with a common heart. The conjoined fetuses were diagnosed as thoracopagus twins, and by means of color Doppler, a single beating heart shared between the thoraxes was demonstrated. At 10 weeks 3 days of gestation, the CT had a spontaneous cardiac arrest confirmed by means of color Doppler.

The subsequent prenatal course was uneventful. A normal healthy child was born at the 39th week of gestation by spontaneous vaginal delivery (weight 2,792 g, male). Vestiges of the CT could not be detected in the appendages.

DISCUSSION

To our knowledge, the present case is the first report of CT occurring in a triplet pregnancy after transfer of two blastocysts obtained by ICSI procedure. Although the origins of CT remain unknown, CT are generally considered to be a variant of MZT. Two theories have been proposed to explain the origins of CT (8). "Fission theory" proposes the incomplete separation of embryonic discs at around 13 to 15 days after fertilization. "Fusion theory" postulates that secondary fusion occurs between two originally separate embryonic discs (9).

As ART has become one of the popular methods to treat infertility all over the world, reported cases of MZT have increased (4, 5, 10, 11). It has been suggested that steps in ART, such as ovulation induction (11), conventional IVF, ICSI, blastocyst culture (4, 5), and assisted hatching (10) may have increased the occurrence of MZT. Similarly, the incidence of CT could be increased by ART. However, because CT are very rare phenomenon, we do not have enough epidemiologic data to understand the true occurrence of CT after ART.

FIGURE 2

Ultrasonographic image of the conjoined twins in a triplet pregnancy. Single fetus (**A**) and conjoined twins (**B**) at 8.0 weeks' gestation.

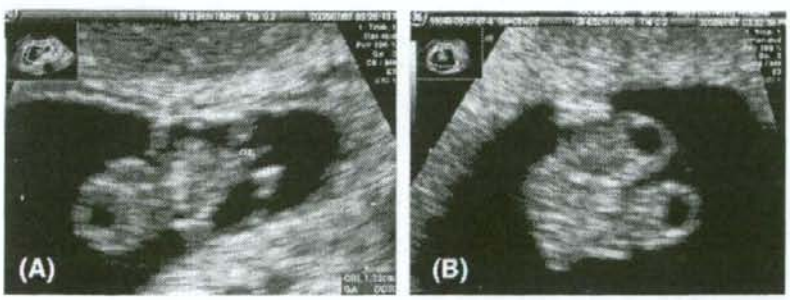

Hirata. Conjoined twins after ART. Fertil Steril 2008.